

CHAPTER TWO

2.0 REVIEW OF LITERATURE

2.1 MATHEMATICAL MODELS OF BLOOD FLOW

One-dimensional mathematical models of vascular blood flow have previously been developed to model flow through relatively simple networks. Olufsen (1999) has formulated a non-linear physiological model predicting blood flow and pressure at any position along the larger systemic arteries. The model parameters are regarded as functions of time and space, hence by definition, the model is two-dimensional, but the model can be restricted to include one spatial dimension (the length of the arteries). She focussed on how to restrict the computational domain while maintaining a physiological approach, that is, on deriving a physiologically correct downstream boundary condition. This allows the model to be implemented and executed without any excessive computational cost. The Olufsen model terminated the large arteries by attaching a structured tree representing the remainder of the arterial system. The model of the large arteries is fully non-linear. Hence, she constructed a semi-analytic solution based on linear hydrodynamic model for the structured tree. To judge the performance of the structured tree model, the Olufsen model made comparison with the pure resistance and Windkessel model (Westerhof *et al.*, 1971). According to the results of their studies, the advantage of both the pure resistance and the Windkessel model is that they are easy to understand and computationally in-expensive, whereas the disadvantage is that they are not able to capture the wave propagation phenomenon in the part of the arterial system. Furthermore, neither the pure resistance nor the Windkessel model could account for the phase lag between flow and pressure. The Windkessel model requires estimates of the total arterial resistance and compliance for each terminal segment, and the pure resistance model needs the total arterial resistance. When the pure resistance and Windkessel model are coupled to the non-linear equations for the larger arteries, both models are able to capture the overall behaviour of the system. Olufsen (1999) compared the impedance boundary condition to a single zero-dimensional electric analog, the Windkessel model and to the resistance boundary condition. The advantage of both the pure resistance and Windkessel models is that they are easy to understand and computationally inexpensive, whereas the disadvantage is that they are not able to capture the wave propagation phenomena in the part of the arterial system that they model. Furthermore, neither the pure resistance nor the Windkessel model can account for the phase lag between flow and pressure. The most striking difference is that the pure resistance model affects the overall shape of the curve. The forced in-phase condition at the outflow boundary results in a narrowing of the width of the loop back through the vessel.

Furthermore, the pure resistance model can be seen as a special case of the Windkessel model incorporating only the DC resistance. For the Windkessel model, flow and pressure are also nearly in phase, but the narrowing is not reflected back through the vessel. Finally, it is observed that the structured tree model does indeed retain some phase lag between flow and pressure. The overall shapes of the pressure profiles are similar, but there are some significant differences. These have to do with the fact that the structured tree model includes wave propagation effects for the entire tree, which the Windkessel model does not. Hence, the Windkessel and pure resistance models are likely to introduce artificial reflections. The reflections from the pressure when the Windkessel model and especially the pure resistance model are used are more pronounced than for the structured tree model.

Smith *et al.* (2002) have developed an anatomically based model of transient coronary blood flow in the heart. They developed an efficient finite difference model of the blood flow through the coronary vessels and applied it to a geometric model of the largest six generations of the coronary arterial network. By constraining the form of the velocity profile across the vessel radius, the three-dimensional Navier-Stokes equations are reduced to one-dimensional equations governing conservation of mass and momentum. These equations are coupled to a pressure-radius relationship characterising the elasticity of the vessel wall to describe the transient blood flow through a vessel segment. The two-step Lax and Wendroff (1960) finite difference method is then used to numerically solve these equations. The flow through bifurcations where three vessel segments join is governed by equations of conservation of mass and momentum. The solutions to these simultaneous equations are calculated using the multi-dimensional Newton-Raphson method.

Olufsen *et al.* (2000) have carried out a numerical simulation and experimental validation of blood flow in arteries with structured-tree outflow conditions. The aim of their work was to develop and use one-dimensional fluid-dynamic model to predicting blood flow and pressure in the systemic arteries at any position along the vessels. Blood flow in the large systemic arteries is modeled using one-dimensional equations derived from the axisymmetric Navier-Stokes equations for flow in compliant and tapering vessels. The arterial tree is truncated after the first few generations of large arteries with the remaining small arteries and arterioles providing outflow boundary conditions for the large arteries. By modeling the small arteries and arterioles as a structured tree, a semi-analytical approach based on a linearised version of the governing equations was used to derive expressions for the root impedance of the structured tree in the frequency domain. In the time domain, this provides the proper outflow boundary condition. The structured tree is a binary asymmetric tree in which the radii of the daughter vessels are scaled linearly with the radius of the parent vessel. Blood flow and

pressure in the large vessels are computed as functions of time and axial distance within each of the arteries. Comparison between the simulations and magnetic resonance measurements in the ascending aorta and nine peripheral locations in one individual shows excellent agreement between the two.

At present, the nonlinear one-dimensional wave propagation method offers an excellent compromise between anatomic accuracy and inclusion of nonlinear advective losses and material properties. However, due to the fact that the vascular system includes billions of blood vessels, these one-dimensional numerical models must invariably be truncated and appropriate outflow boundary conditions specified. Ideally, these numerical models can be terminated at a level where the nonlinear losses are minor and simpler, linear models are adequate to describe flow velocity and pressure waves. Stergiopoulos *et al.* (1992) used a lumped parameter model to account for the capacitive and resistive effects of the vasculature at the exits of a one-dimensional wave propagation model. Formaggia *et al.* (2001) studied wave propagation and reflection due to stenting, using finite elements to solve the one-dimensional nonlinear equations of blood flow, a prescribed pressure at the inlet, and a non-reflecting outlet boundary condition representing a tube of infinite length. Olufsen (1999) described a combined one-dimensional wave transmission and impedance approach whereby a finite difference method is used to solve the nonlinear wave transmission equation in a model of the major arteries and Womersley's elastic vessel theory is employed on a fractal branched network to represent the distal vascular beds for each of the outlets of the numerical domain.

Vignon and Taylor (2004) have previously described a method to solve the one-dimensional nonlinear equations of blood flow in elastic vessels utilizing space-time finite element method with Galerkin/least-squares (GLS) stabilization using resistance and impedance outlet boundary condition. They described a new approach, the "coupled multidomain method" based on a conservation form of the one-dimensional equations of blood flow and a consistent treatment of various outlet boundary conditions through an integral boundary term that represents the downstream analytic domain. The outlet boundary conditions are derived following an approach analogous to the Dirichlet-to-Neumann (DtN) method (Givoli, 1992). In the downstream domain, they solved the simplified zero/one-dimensional equations to derive relationships between pressure and flow accommodating periodic and transient phenomena. They also presented a new boundary condition that accommodates transient phenomena, based on a Green's function solution of the linear damped wave equations in the downstream domain.

2.2 STROKE AND DIAGNOSIS

The definition of stroke used for epidemiological studies is based on clinical presentations of WHO (1988); Anderson and Stewart-Wynne (1991); Bamford (1992); Harrison, (1980). Since the advent of computed tomography (CT) Scan and Magnetic Resonance Imaging (MRI), greater attention has been focused on changes in the occurrence and case-fatality of the different pathological types of stroke. Although the criteria for the definition of stroke are relatively accurate for determining the presence or absence of stroke, the differentiation of pathological types requires brain imaging (Von et al, 1981; Shinar *et al.*, 1985; Gross *et al.*, 1986). Experience from population-based studies has shown that up to a quarter of all stroke events are treated at home or in community-based long-term care institutions, making the differentiation of stroke type's very difficult (Bonita *et al.*, 1984; Anderson et al, 1993; Asplund *et al.*, 1995). Nevertheless, the ability to classify stroke into hemorrhagic and ischemic types in epidemiological research would improve understanding of the nature of stroke and provide clues to its etiology and potential interventions in the acute stage (Hawkins *et al.*, 1995).

To achieve this goal in the absence of diagnostic investigations, clinical scoring protocols have been produced by Allen (1983) and Poungvarin *et al.* (1991). These two scoring protocols are the only ones currently available that have been validated against both postmortem and CT scan results. They are designed to give an objective score based on clinical variables shown to be significantly different for hemorrhagic and ischemic strokes. Hawkins *et al.* (1995) have tested these two clinical scores in a subset of patients from a large population-based stroke study to examine the feasibility of applying one of the scores to the whole data set to allow differentiation between hemorrhagic and ischemic stroke.

Disabling stroke is already prevalent in rural South Africa as in high-income countries (SASPI, 2004). Furthermore, the burden of stroke is likely to increase in South Africa and across sub-Saharan Africa as a result of an anticipated demographic and health transition (Yusuf *et al.*, 2001). Yet, despite the growing burden of stroke, there are very few computed tomography scanners in Sub-Saharan Africa (SSA), and the vast majority of patients with stroke do not have access to brain imaging (El Khamlichi, 2001). Because the shortage of brain imaging facilities in the region is most unlikely to be resolved in the near future, it is of practical importance to know if clinical stroke scores enhance the clinicians' bedside assessment of pathologic stroke type in SSA. Although two small retrospective studies have assessed the Siriraj Stroke Score (SSS) in Nigeria and Ethiopia, no prospective studies have

assessed either the SSS or the Guy's Hospital Stroke Score (GHSS) in SSA (Ogun *et al.*, 2002; Zenebe *et al.*, 2005).

Connor et. al. (2007) in their study could not directly extrapolate the results from validation studies undertaken in populations outside SSA. First, because many of the scores used to distinguish pathologic stroke type use "atheroma markers" such as angina, intermittent claudication, diabetes, and myocardial infarction (Allen, 1983; Poungvarin *et al.*, 1991), the population does not have a high prevalence of extracranial atherosclerotic disease either in the general population or in patients with stroke (Van der Horst, 1984; Mollentze, 2004). Second, the prevalence of intracerebral hemorrhage may be very different (Rosman, 1986). Although there are several scores available, they chose to use the SSS and Guy's Hospital Stroke Score because these required the least ancillary testing and investigation and appeared to be the simplest to use (Allen, 1983; Poungvarin *et al.*, 1991). The SSS only requires a history and examination, whereas the GHSS requires a chest x-ray and electrocardiogram in addition. They felt these scores were the most likely to succeed in settings where resources are scarce.

Connor *et al.* (2007) also assesses the accuracy of the GHSS and SSS in distinguishing between intracranial hemorrhage (cerebral hemorrhage and subarachnoid hemorrhage) and ischemic stroke in black patients with stroke in South Africa. Later in the study, they assessed whether the scores were more accurate than clinicians in distinguishing pathologic stroke type. Neither score offered much advantage over their stroke team clinicians' assessment of pathological stroke type. They found out that the SSS and GHSS did not perform at all well in diagnosing the pathologic stroke type in black South African patients with stroke. The SSS performed marginally better than the GHSS and had much higher sensitivity for detecting intracranial hemorrhages. But when they compared their findings with those found in Nigeria and Ethiopia, they found a higher sensitivity, specificity, and positive predictive value for the SSS in detecting intracranial hemorrhage than was found in Nigeria and Ethiopia.

Routine computed tomography for all patients with stroke is not available to some doctors, and this poses management problems (Logan *et al.*, 1994). The Guy's Hospital score and the Siriraj score are the "poor man's computed tomography" in terms of reliability, but Celani *et al.* (1994) suggested that they may be used as a temporary guide to management pending computed tomography, and Poungvarin *et al.* (1991) suggested that they could be used as a means of targeting computed tomography at cases in which uncertainty exists (Poungvarin *et al.*, 1991). If computed tomography is not available at all (for whatever reason), or if the 10-14 days after stroke during which computed tomography can reliably differentiate infarction

from haemorrhage has passed, the Guy's Hospital and Siriraj scores may still have a useful function.

If one considers, for example, the age group 75- 84 (the decade in which stroke is most common) and allows for the difference in 30 day mortality between haemorrhage and infarction (Bamford, *et al.*, 1990), roughly 8% of the patients surviving to 30 days would be expected to have had a cerebral haemorrhage. Aspirin after ischaemic stroke can be expected to prevent 40 vascular events per 1000 patients treated for three years (Antiplatelet Trialists, 1994). If all patients surviving to 30 days are given aspirin and it is assumed that giving aspirin to patients with haemorrhagic stroke will cause rebleeding in all cases within three years, then 80 cerebral haemorrhages will be induced per 1000 patients treated for three years. If the chance that the original stroke was haemorrhagic was 50% according to one of the scoring systems then a breakeven point exists. This corresponds to a Guy's score of 14 or a Siriraj score of approximately 0.5.

Logan *et al.* (1994) therefore suggested that patients surviving to 30 days who score below these values could be given aspirin while those scoring above these values should not. On the basis of validation work done in Britain on the Guy's score (Sandercock *et al.*, 1985a) this would deprive about 5% of patients with infarcts of aspirin treatment, resulting in an increase of only about two preventable events per 1000 patients per three years. Delaying aspirin treatment for 30 days may also result in an increase in some preventable events, it is difficult to calculate how many and the number is probably not great, but it is probably best to delay aspirin for 14 days anyway. The assumption that aspirin will cause rebleeding in all cases of haemorrhagic stroke is almost certainly pessimistic as it is based on the axiom "first of all do no harm."

Haemorrhagic and ischaemic stroke cannot be distinguished clinically with a simple clinical evaluation, and it is virtually impossible for all stroke patients to have a computed tomography scan immediately after admission. Thus, in small district hospitals as well as in large university centres, the weighted clinical score may offer some advantages to physicians who are involved in stroke management and need to distinguish between haemorrhage and ischaemia for the purpose of treatment. The Allen score has been validated in different European settings (Sandercock *et al.*, 1985b; Celani *et al.*, (1992), and has a reasonably good (90%) accuracy when the suggested cutoffs (less than four (4) for ischaemia and less than twenty four (24) for haemorrhage) are used; however, it requires several historical and clinical details to be registered and cannot be used until 24 hours after the stroke. The Siriraj score is

much easier to determine, and can be used immediately after the stroke; however, it has been tested only in Thailand, where the pretest probability of haemorrhage is higher than in Europe; as the positive predictive value depends on prevalence, the score needs to be validated in Europe to check the predictive values. In a different work to further validate the Siriraj score in Europe, Celani *et al.* (1994) compared Allen and Siriraj scores in Italy. They carried out several analyses, and in 231 cases, they found out that the prevalence of haemorrhage (diagnosed with computed tomography) was 14.7% (95% confidence interval 10.1% to 19.3%). The overall comparability of the Allen and Siriraj scores was fair. The Allen score was uncertain in 44 cases, and the Siriraj score was uncertain in 38; however, kappa statistic showed a worse comparability between the two scores in terms of certain results. When only the results that were within the diagnostic range with both the scores (164 cases) were considered, the agreement in diagnosing infarction and haemorrhage was high. When computed tomography scan results are used as a standard, the diagnostic gain for detecting haemorrhage was 0.58 with the Allen score and 0.48 with the Siriraj score; however, for the detection of infarction, besides a poor diagnostic gain (0.05 and 0.08), the positive predictive value was 91% for the Allen score and 93% for the Siriraj score. In the 157 patients in whom the two scores were both certain and in agreement, when the combined result was compared with results of computed tomography, accuracy was slightly better (0.92), and the diagnostic gain was 0.6.

Stroke is the most common neurological disorder causing death or disability among adults in industrialized nations. Ischemic events account for approximately 85% of all strokes, and hemorrhages account for approximately 15% (Bamford *et al.*, 1990). The management of the two disorders differs substantially, and therefore the differentiation of cerebral infarction (CI) and cerebral hemorrhage (CH) and the identification of stroke complications are important in acute stroke. A reliable differentiation is not possible on the basis of clinical examination alone. Even sophisticated clinical stroke scoring systems for the differential diagnosis of infarct versus hemorrhage revealed a poor accuracy (Weir *et al.*, 1994; Hawkins *et al.*, 1995). At present, one of the most accurate methods of distinguishing cerebral hemorrhage from infarction is CT (Sandercock *et al.*, 1985b). Although CT is very sensitive in the detection of intracerebral hemorrhage, it can be inconclusive in early stages of cerebral ischemic infarction (Bryan *et al.*, 1991; Lindgren *et al.*, 1994). CT currently also serves to identify important stroke complications.

Depending on local conditions, ready access to CT facilities on admission may not be available everywhere. Large population-based studies revealed that approximately one third

of the patients with acute stroke had no CT before treatment was started, and this applied even to centers experienced with stroke management (Bamford *et al.*, 1990).

CT scanning is important to identify stroke pathology and exclude mimics. Its poor availability in our environment makes the search for simple, reliable clinical-score imperative. A study which aims at validating the SSS and determine the discriminant values of its parameters in the black population of African-Nigerians was carried out by Kolapo *et al.* (2006). A prospective multicenter study was carried out on patients that presented with stroke and had brain CT scan done within 14 days of onset. This preliminary study has shown that only 9% of our hospital stroke population had benefit of CT scan. The limited number of patients studied and their potential lack of representativeness, represent a funding issue to properly establish the performance of clinical scoring systems and assist in descriptive epidemiology of hospital and community-based stroke studies in resource-poor settings. However, in this study, the SSS diagnosis correlates significantly with CT diagnosis.

Also in their work to validate the SSS in the North-Eastern Nigeria, Nyandaiti and Bwala (2008) enrolled patients who had stroke less than fourteen days before admission into the study. Clinical variables for calculating the Siriraj stroke score were documented all patients subsequently had computerized tomography scan performed. A total of fifty patients were studied from University of Maiduguri Teaching Hospital and the State Specialist Hospital Maiduguri. Twenty-seven (27) patients had infarction while twenty-three (23) patients had hemorrhagic strokes respectively, based on the CT scan findings. The Siriraj stroke score correctly diagnosed fourteen (14) as infarction and twenty (20) as having hemorrhagic strokes; sixteen (16) subjects were unclassified. The SSS correctly diagnosed thirteen (13) cases as infarctive and seventeen (17) as hemorrhagic strokes as confirmed by CT scan. The sensitivity and the predictive value of the SSS were 76.2% and 93% for infarction and 94.4% and 85% for hemorrhagic stroke respectively with overall accuracy of 84.6%. The clinical variables such as headache, vomiting and atheroma markers did not show discriminant value independently in differentiating CI and CH. However, level of Consciousness (coma) and diastolic blood pressure of greater than 110 mmHg are discriminant variables in differentiating CI and CH. They concluded that SSS score is recommended to be used in this community especially where CT scan is not available or affordable and the physician wishes to start thrombolytic and/or anticoagulation therapy.

Maurer *et al.* (1998) in their study tried to assess the sensitivity and the specificity of Transcranial color-coded duplex sonography (TCCS) in the differentiation between intracerebral hemorrhage and ischemic stroke and to examine whether intracerebral

complications of cerebrovascular diseases can be detected. TCCS is a diagnostic tool that allows a 2-dimensional imaging of brain parenchyma and a color-coded imaging of the intracranial vessels (Lindner *et al.*, 1995). The method is noninvasive and mobile, and bedside examination is feasible. Previous studies have shown that TCCS permits the detection of intracerebral hemorrhages and intracerebral vessel occlusions (Seidel *et al.*, 1993; Becker *et al.*, 1993; Seidel *et al.*, 1995). TCCS is currently being applied only in a few centers, but ultrasound systems suitable for TCCS can widely be available even in general hospitals. But just like CT scan equipments, these are equipments not generally available in a lot of hospitals, because of its cost implications.

2.3 THE BLOOD GLUCOSE-INSULIN SYSTEM

The glucose-insulin system is an example of a closed-loop physiological system. A healthy person, normally has a blood glucose concentration at about 70 – 110 mg/dL . The glucose-insulin system helps us to keep this steady state. In Figure 2.1 a simple description of the system is shown. Most of the time, healthy person is in the green area, having normal blood glucose concentration.

If the person ingests additional glucose to the system e.g via a meal, the person moves to the red area, with a higher blood glucose concentration. When this happens a signal is sent to the pancreas, which β -cells react by secreting the hormone insulin. This insulin increases the uptake of glucose by the cells, liver etc. and brings the person back in the green area. If the blood glucose concentration goes below the normal level, the person is in the blue area. This could happen as a response to exercise, which increases the glucose uptake. When the person is in the blue area with low blood glucose concentration a signal is also send to the pancreas. The pancreas α -cells react by releasing glucagon. This glucagon affects the liver cells to release glucose in to the blood until the person is back in the green area again (Li *et al.*, 2006). This is a very simple description of a more complicated system. But it is this simplistic way of explaining the metabolism.

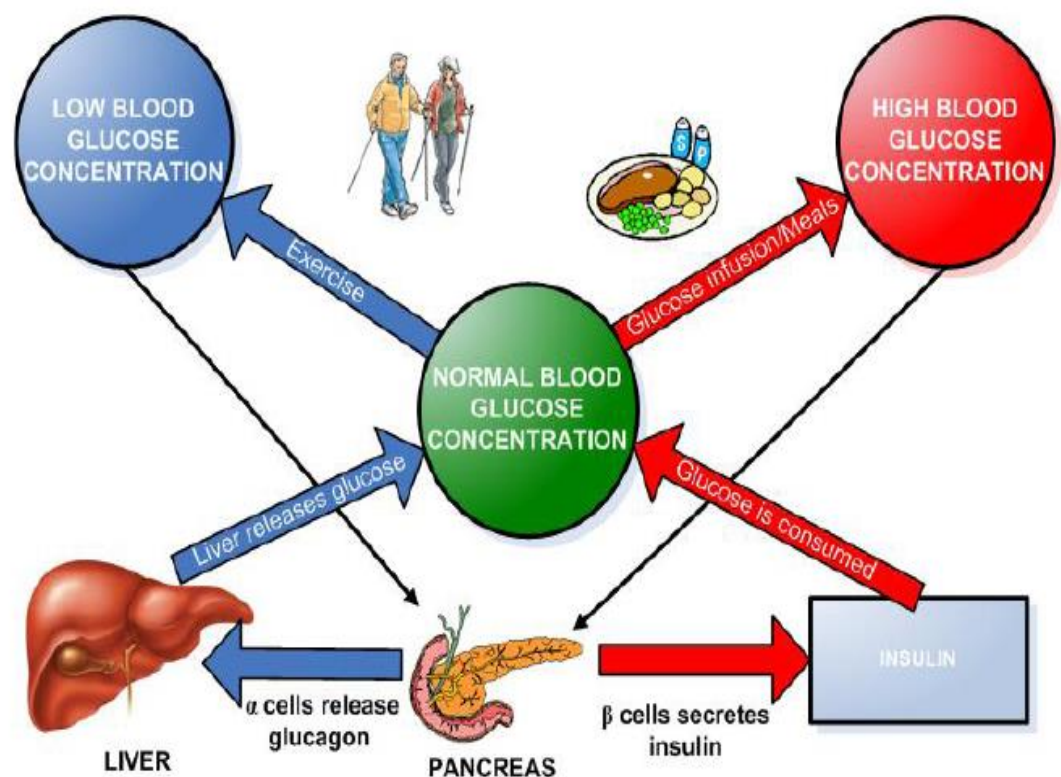


Figure 2.1: The Blood Glucose-Insulin System

2.3.1 Hyperglycemia

A person has hyperglycemia, when the blood glucose level is above 270 mg/dL . This can arise e.g. when a diabetic eats a large meal or has a low level of insulin in the blood. Hyperglycemia is extremely dangerous if not treated.

2.3.2 Hypoglycemia

A person has hypoglycemia when the blood glucose level is below 60 mg/dL . This can happen e.g. after too much exercise, a too large insulin dosage, small amount of carbohydrates in the food or if the diabetic skips meals. Hypoglycemia can result in loss of consciousness. Avoiding hypoglycemia is an important issue when you are using insulin as treatment.

2.4 MATHEMATICAL MODEL OF GLUCOSE – INSULIN METABOLISM

A correct glucose metabolism is one of the key factors in keeping a healthy state in mammals. Among other processes, this is accomplished mostly via regulatory action of hormones released by specific cell population inside the pancreas. A very relevant role is played in this process by the hormone, insulin, synthesized by the pancreatic cells. The normal blood glucose concentration level in humans is in a narrow range (70–110 mg/dl) (Makroglou *et al.*, 2005). Exogenous factors that affect the blood glucose concentration level include food intake, rate of digestion, exercise, reproductive state, etc. The pancreatic endocrine hormones, insulin and glucagons, are responsible for keeping the glucose concentration level in check.

Several attempts at building a satisfactory model of the glucose-insulin system are recorded in the literature. The minimal model, which is the model currently and mostly used in physiological research on the metabolism of glucose, was proposed in the early eighties for the interpretation of the glucose and insulin plasma concentrations following the intra-venous glucose tolerance test (IVGTT) (Shen *et al.*, 1970). Himsworth (1936) identified two different types of diabetes mellitus: the insulin-sensitive and the insulin-insensitive types, by using an insulin-glucose test. Since then, several other methods have been used to quantify insulin action. The tests that have been used to assess insulin sensitivity include: insulinogenic ratio (insulin/glucose) (Gaetano and Arino, 2002), glucose/insulin ratio (Seltzer *et al.*, 1967), glucose clamp technique (DeFronzo *et al.*, 1979), frequently sampled intravenous glucose tolerance test (FSIGT) (Kahn *et al.*, 1994) and minimal model technique (Bergman and Cobelli, 1980). Another simple and reliable test, the short insulin tolerance test (SITT), was developed by Bonora *et al.* (1989). There has been no model study, as far as the authors are

aware, on glucose disappearance from blood plasma in Nigerians. However, a glucose disappearance study on Nigerians was carried out by Fasanmade (1987) using the short insulin tolerance test. No models were developed in that study and glucose disappearance rate constants were determined using the least square method on patient data.

Insulin, the primary anabolic hormone of the human body, has been implicated in the aetiopathogenesis of several non-communicable disease like hypertension, peripheral vascular disease, coronary heart disease and even cancer (Bakari, 2004). Measurement of insulin resistance, a measure of glucose disappearance rate, has been reported by Mari *et al.* (2001) to be of interest in clinical investigation of diabetes and hypertension. It was apparent that insulin secretion is associated with energy abundance (Guyton and Hall, 1996). That is, when there is great abundance of energy-giving foods in a diet, especially excess amounts of carbohydrates and proteins, insulin is secreted in great quantity. This is especially true for excess carbohydrates, less for excess proteins, but only slightly even for fats. Although insulin plays a role in carbohydrate, proteins and fats metabolism, this study has been narrowed down to the modeling of glucose (carbohydrate) metabolism, following the short insulin tolerance test (Bonora *et al.*, 1989). Diabetes mellitus is a disease of the glucose-insulin regulatory system (Bergman *et al.*, 2002; Topp and Finegood, 2000), which is referred to as hyperglycemia. Diabetes is classified into two main categories: Type 1 diabetes, juvenile onset and insulin-dependent, and Type 2 diabetes, adult onset and insulin-independent. Type 1 diabetes is caused by deficiency of circulating insulin due to the loss of insulin producing β -cells in the Langerhans islets of the pancreas (Makroglou *et al.*, 2005), while Type 2 diabetes is caused by the failure of pancreatic beta cells to respond appropriately to the prevailing blood glucose levels (Bakari and Onyemelukwe, 2005). Complications of the disease include retinopathy, nephropathy, peripheral neuropathy and blindness (Derouich and Boutayeb, 2002). The ability of insulin to lower blood glucose is referred to as Insulin Sensitivity (IS), while Glucose Effectiveness (GE) is a measure of the fractional ability of glucose to lower its own concentration in plasma independent of increased insulin (DeFronzo and Ferrannini, 1991). To this day, the standard treatment for Type 1 diabetes mellitus is the administration of exogenous insulin to mimic the normal metabolic regulatory system in healthy subjects. Insulin facilitates cellular glucose uptake and stimulates conversion of glucose into glycogen (Gerich, 1993).

In summary, it can be concluded that the literature on blood flow model is deficient in the following areas; all the models developed have no ability of capturing discontinuity in flow and none was applied to disease situation. All the authors modeled normal situation and this research project would attempt to model disease situation by doing the following: developing

a numerical model to solve the developed blood flow equations. For example, in the presentation of numerical model of solution of blood flow in the next section, we will use the finite volume method and the Roe Riemann concept to solve the developed blood flow model to allow for discontinuity in flow situations. This will allow the model to capture disruption in blood flow.

The literature on Glucose and Insulin model is deficient in the following areas; all the models developed are kinetic models; kinetic models describe quite well, the short term dynamics of glucose steady state level only and provide no pathway for diabetes development. Secondly pressure drop considerations cannot be captured by kinetic model and this research would attempt to model the glucose-insulin system as the gut and blood systems. For example in the representation of the model, the gut and blood system is modeled as a model of mixed flow tanks in series. The coupling of reaction rates and molecular diffusion and transport is significantly dependent on absorption and diffusion, which the kinetic model did not address. Once disease situation can be captured, software program can be written, which will help in designing therapy by clinicians to treat patient. This software will be a visual aid that will allow medical experts see condition of patients on computer screen. This software will also be capable of guiding the medical experts in treatment procedures by presenting to the medical experts the situation of patient.

2.4.1 Brief History of Insulin

Insulin was first isolated from the pancreas by Banting and Best (1922), and almost overnight the outlook for the severely diabetic patients changed from one of rapid decline and death to that of a nearly normal person (Guyton and Hall, 1996). Historically, insulin has been associated with “blood sugar” and true enough, insulin has profound effects on carbohydrate metabolism. Yet it is abnormalities of fat metabolism, causing such conditions as acidosis and arteriosclerosis, which are the usual causes of death of a diabetic patient. Also, in patients with prolonged diabetes, diminished ability to synthesize proteins leads to wasting of the tissues as well as many cellular functional disorders. Therefore, it is clear that insulin affects fat and protein metabolism almost as much as it does carbohydrate metabolism.

2.4.2 Physiologic Anatomy of the Pancreas

The pancreas is composed of two major types of tissues: the *acini*, which secrete digestive juices into the duodenum, and the *Islet of langerhans*, which do not have any means of emptying their secretions externally but instead secrete insulin and glucagon directly into

the blood. The pancreas of the human being has 1 to 2 million islets of langerhans, each only about 0.3 millimeter in diameter and organized around small capillaries into which its cells secrete their hormones. The islets contains three major types of cells, *alpha, beta and delta cells*, which are distinguished from one another by their morphologic and staining characteristics. The beta cells, consisting about 60 percent of all the cells, lie mainly in the middle of each islet and secrete insulin. The alpha cells, about 25 percent of the total, secrete *glucagon*. And the delta cells about 10 percent of the total secrete *somatostatin*. In addition, at least one other type of cell, the pancreatic polypeptide (PP) cell, is present in small numbers in the islets and secretes a hormone of uncertain function called *pancreatic polypeptide*. The close interactions among these cell types in the islets of langerhans allow direct control of secretion of some of the hormones by the other hormones. For instance, insulin inhibits glucagon secretion, and somatostatin inhibits the secretion of both insulin and glucagon (Guyton and Hall, 1996).

2.4.3 Insulin and Its Metabolic Effects In Human

The normal blood glucose concentration level in human is in a narrow range (70 – 110 mg/dl) (Makroglou and Kuang, 2005). Exogenous factors that affect the blood glucose concentration level include food intake, rate of digestion, exercise, reproductive state. The pancreatic endocrine hormones insulin and glucagon are responsible for keeping the glucose concentration level in check. Roughly speaking, insulin and glucagon are secreted when the blood glucose concentration level is high and low respectively. When the level is high, the beta (β)-cells release insulin which results in lowering the blood glucose concentration level by inducing the uptake of the excess glucose by the liver and other cells (e.g muscles) and by inhibiting hepatic glucose production. When the blood glucose level is low, the alpha (α)-cell release glucagon; which results in increasing the blood glucose level by acting on liver cells and causing them to release glucose into the blood. If one's glucose concentration level is constantly out of the range (70 – 110 mg/dl), this person is considered to have blood glucose problem known as hyperglycemia or hypoglycemia. Diabetes mellitus is a disease of the glucose-insulin regulatory system which is referred to as hyperglycemia.

Diabetes is diagnosed when the person has the symptoms of diabetes (such as polyuria, unexplained weight loss and excess thirst) and a casual plasma glucose level out of the normal range (Watson, 2005). Casual refers to the fact that the blood sample has been taken at any time of the day regardless of the last meal.

There are two principal types of diabetes which have different aetiologies. Type 1 or *insulin-dependent* diabetes mellitus (IDDM) is caused by the destruction of β -cells in the islet of

langerhans. The destruction is an auto-immune response associated with environmental and genetic factors. This process starts early in life and it may be several years before symptoms begin to appear. The onset can then be very rapid.

Type 2 or *non-insulin dependent* diabetes mellitus (NIDDM) covers a multitude of different disorders. The basic problem is that either the islets of langerhans gradually diminish their insulin output or there is increased peripheral resistance to the action of insulin. The onset tends to be slow. Obesity and lack of exercise are the commonest causes of insulin resistance and hence of type 2 diabetes. The most common age of onset is 50-70 years. There is a strong genetic influence, and as a result certain families and ethnic groups are much more likely to have type 2 diabetes (Watson, 2005). For example in Nigeria about 1-2 percent of the population are believed to be diabetic most of whom (greater than 90 percent) have the insulin dependent diabetes mellitus (NIDDM) type (Fasanmade, 1987). The pathogenesis of type 2 diabetes is still not clearly understood and various potential causes are usually investigated through complex in vitro or in vivo experimentation (Thomaseth *et al.*, 2003).

Insulin is prescribed for all insulin-dependent diabetics (Watson, 2005). Non-insulin-dependent diabetics may require insulin during periods of stress (e.g infection, surgery, pregnancy or emotional crisis). Insulin is prescribed for the individual whose plasma glucose level cannot be controlled at acceptable levels despite weight control and adherence to dietary regulation, and for the treatment of ketoacidosis and non-ketotic hyperglycemia.

2.4.4. Chemistry of Insulin

Insulin is a small protein; human insulin has a molecular weight of 5808. It is composed of two amino acid chains, shown in Figure 2.2, connected to each other by disulfide linkages. When the two amino acid chains are split apart, the functional activity of the insulin molecule is lost.

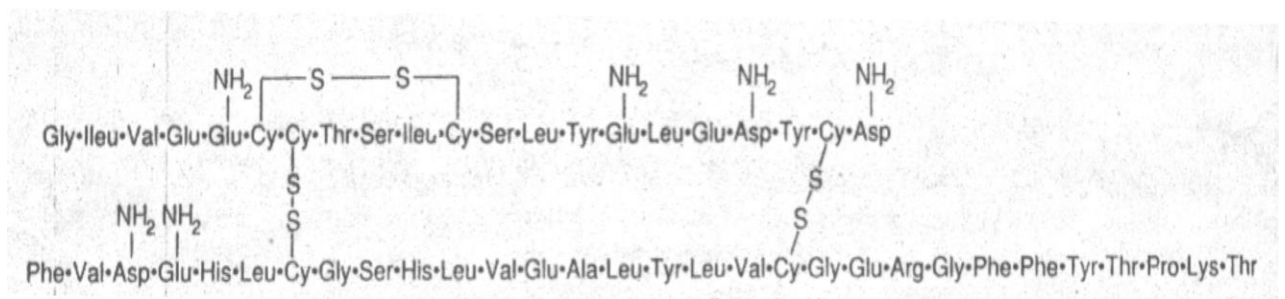


Figure 2.2: Human Insulin Molecules
(Guyton and Hall, 1996).

Insulin is synthesized in the beta cells by the usual cell machinery for protein synthesis, beginning with translation of the insulin ribonucleic acid (RNA) by ribosome attached to the endoplasmic reticulum to form an *insulin prepro-hormone*. This initial preprohormone has a molecular weight of about 11,500 but it is then cleaved in the endoplasmic reticulum to form a proinsulin with a molecular weight of about 9000; most of this is further cleaved in the Golgi apparatus to form insulin before being packaged in the secretory granules. However, about one sixth of the final secreted product is still in the form of proinsulin. The proinsulin has virtually no insulin activity (Guyton and Hall, 1996). When insulin is secreted into the blood, it circulates almost entirely in an unbound form; it has a plasma half-life that averages only about 6 minutes, so that it is mainly cleared from the circulating within 10 to 15 minutes. Except for that portion of the insulin that combines with receptors in the target cells, the remainder is degraded by enzyme insulinase mainly in the liver, to lesser extent in the kidneys and muscle, and slightly in most other tissues. This rapid removal from the plasma is important because at times, it is equally as important to turn off rapidly as to turn on the control functions of insulin.

To initiate its effects on target cells, insulin first binds with and activates a membrane receptor protein that has a molecular weight of about 300,000. It is the activated receptor, not the insulin that causes the subsequent effects.

2.4.5 Actions of Insulin

Insulin may be prepared from the pancreas of pigs (rarely from beef) or, most commonly, synthetically by genetic engineering (Watson, 2005). Because it is a protein, insulin is destroyed in the gastrointestinal tract by proteinases; therefore, it must be given parenterally. Several types are available and may be classified as *rapid-acting* with a shorter duration of action, as *intermediate-acting* with a longer duration of action, or as *long-acting* with a prolonged duration of action. The rapid-acting preparations include unmodified, clear solutions such as soluble insulin. The intermediate-acting insulin include isophane insulins and insulin zinc suspensions. Long-acting insulins, which have an extended effect on lowering blood glucose, are mostly prolonged action insulin zinc suspensions. In addition, biphasic insulins are available which are mixtures of rapid-acting and long-acting insulin. The use of two different insulins has the advantage of combining an intermediate effect with a more long-lasting sustained effect. Commonly used biphasic insulins include humalog mix 25 (25% insulin lispro, 75% insulin lispro protamine), Human mixtard (soluble and isophane insulin) and humulin (soluble insulin and isophane insulin). Human mixtard and humulin are differentiated by the different recombinant technologies used in the production of the

isophane insulin. Each is available in different proportions of the two types of insulin it contains.

The main actions of insulin are:

1. Stimulates glucose uptake by cells, thereby making it available for energy production.
2. Increases the storage of glucose as glycogen in liver and muscle.
3. Inhibits release of glucose from glycogen store.
4. Stimulates conversion of glucose into glycerol, which then combines with fatty acids to form triglycerides which are stored in adipose (fatty) tissue.
5. Increases uptake of amino acids by cells and hence facilitates protein synthesis.

2.4.6 Administration of Exogenous Insulin

Insulin is measured in units. Each person's regimen is determined individually in relation to a particular schedule and diet plan in an attempt to achieve a normal physiological level of glucose throughout a 24 hour period. The regimen is organized so that insulin action coincides with major meals and also provides action overnight (Watson, 2005).

The standard treatment for IDDM is the subcutaneous administration of exogenous insulin to mimic the normal metabolic regulatory system in healthy subjects (Clausen *et al.*, 2006).

Several groups of drugs are used in conjunction with dietary control in the treatment of NIDDM. Avoidance of accidental hypoglycemia is a high priority which ever drug is used. The term non-insulin dependent diabetes is misleading as up to 50% of patients with type 2 diabetes ultimately require insulin therapy (Watson, 2005). The main drugs used are described below.

Sulphonylureas: They simulate the β -cells in the islet of langerhans to secrete more insulin and as a result can be very effective in reducing blood glucose levels in the early part of the disease. Commonly used examples are gliclazide, glipizide and glibenclamide, although the latter readily causes hypoglycemia if taken in excess.

Biguanides: The biguanides act by reducing the production of glucose in the liver and increasing glucose uptake in muscle. The person has to be manufacturing at least some insulin for these drugs to work.

α -Glucosidase Inhibitors: Intestinal enzymes known as α -glucosidase are important in breaking down carbohydrates molecules into short sugar chains. Competitive inhibition of these enzymes has a mild effect in reducing blood glucose level.

Meglitinides: The first drug in this group to be used in the UK is repaglinide, which is a derivative of glibenclamide. It is taken just before a meal, has a short duration of action and can be used with metformin.

2.4.7 Distribution and Degradation of Insulin in the Body

Insulin circulates in blood as free monomers, and its volume of distribution approximates the volume of the extra cellular fluids. Under fasting conditions, the pancreas secretes about $40 \mu\text{g/l}$ unit (U) of insulin per hour into the portal vein, to achieve the concentration of 2 to 4 $\mu\text{g/ml}$ (50 to 100 $\mu\text{U/ml}$) and in the peripheral circulation of $0.5 \mu\text{g/ml}$ ($12 \mu\text{ml}$) or about 0.1 nM after meal there is rapid rise in basal level of insulin. Half life is 5 to 6 minutes in normal patient and diabetic patient. This is increased in patient with complicated diabetes mellitus and in insulin resistance diabetes mellitus (with anti-insulin antibodies) $t_{1/2}$ is 17 minutes. Degradation occurs mostly in the kidney, liver and muscles. But 50% of insulin that reaches the liver are destroyed and never reaches the systemic circulation. In terms of duration of action, they are classified as short acting(soluble and semi lente), intermediate/medium(neutral protamine hagedorn- NPH and lente) .long acting (PZI and untalente) with duration of action ranging from 10-36 hours and peak action varying from 4-20 hours. They are usually marked as U40 (40 U/ml), U80 (80 U/ml) and U100 (100 U/ml) and sometimes U500 (500 U/ml). The secretion of insulin is about 30 U/day, however most patients would require more because of the presence of antibodies or insulin resistance due to obesity or stress e.g. infection, ketoacidosis etc. Usually given subcutaneously but can be given intramuscularly or intravenously in emergency.

The relative interaction and contribution in the pathogenesis of this disease of various defects of the glucose-insulin regulatory system associated]for example with β -cells mass, the responsiveness level of β -cells to glucose and the sensitivity of tissues to insulin, remains to be clarified. Complications of the disease include retinopathy, nephropathy, peripheral neuropathy and blindness. There are many diabetic patients in the world and diabetes mellitus is becoming one of the worst diseases with respect to the size of the affected population. This motivates many researchers to study the glucose-insulin endocrine regulatory system. Exogenous factors that affect the blood glucose concentration level include food intake, rate of digestion, exercise, reproductive state. The pancreatic endocrine hormones insulin and glucagons are responsible for keeping the glucose concentration level in check. Insulin and glucagons are secreted from β -cells and α -cells respectively, which are contained in the so-called Langerhans islets scattered in the pancreas. When the blood glucose concentration level is high, the β -cells release insulin which results in lowering the blood glucose concentration level by inducing the uptake of the excess glucose by the liver and other cells

(e.g., muscles) and by inhibiting hepatic glucose production. When the blood glucose level is low, the α -cells release glucagons, which results in increasing the blood glucose level by acting on liver cells and causing them to release glucose into the blood. If one's glucose concentration level is constantly out of the range (70–110 mg/dl), this person is considered to have blood glucose problems known as diabetes mellitus (either hyperglycemia or hypoglycemia).

2.4.8 Effect of Insulin On Carbohydrate Metabolism

Insulin plays a pivotal role in glucose homeostasis by virtue of its ability to inhibit hepatic glucose production and stimulate glucose uptake. The magnitude of these insulin effects depends on the concentration of insulin at the liver site and in the interstitial fluids, respectively. To fulfill its pre-eminent function of regulating glucose metabolism, insulin secretion must not only be quantitatively appropriate but also have quantitative, dynamic properties that optimize insulin action on target tissues (Caumo and Luzi, 2003).

2.4.9 Effect of Insulin in Promoting Glucose Metabolism in Muscle.

During much of the day, muscle tissue depends not on glucose for its energy but on fatty acids. The principal reason for this is that the normal resting muscle membrane is only slightly permeable to glucose except when the muscle fibers are stimulated by insulin; between meals, the amount of insulin that is secreted is too small to promote significant amounts of glucose entry into the muscle cells. However, there are two conditions when the muscles do use large amounts of glucose. One of these is during moderate or heavy exercise. This usage of glucose does not require large amounts of insulin because exercising muscle fibers, for reasons not understood, become permeable to glucose even in the absence of insulin because of the contraction process (Guyton and Hall, 1996).

The second condition for muscle usage of large amounts of glucose is during the few hours after a meal. At this time the blood glucose concentration is high; the pancreas is secreting large quantities of insulin. The extra insulin causes rapid transport of glucose into the muscle cells. This causes the muscle cell during this period to use glucose preferentially over fatty acids.

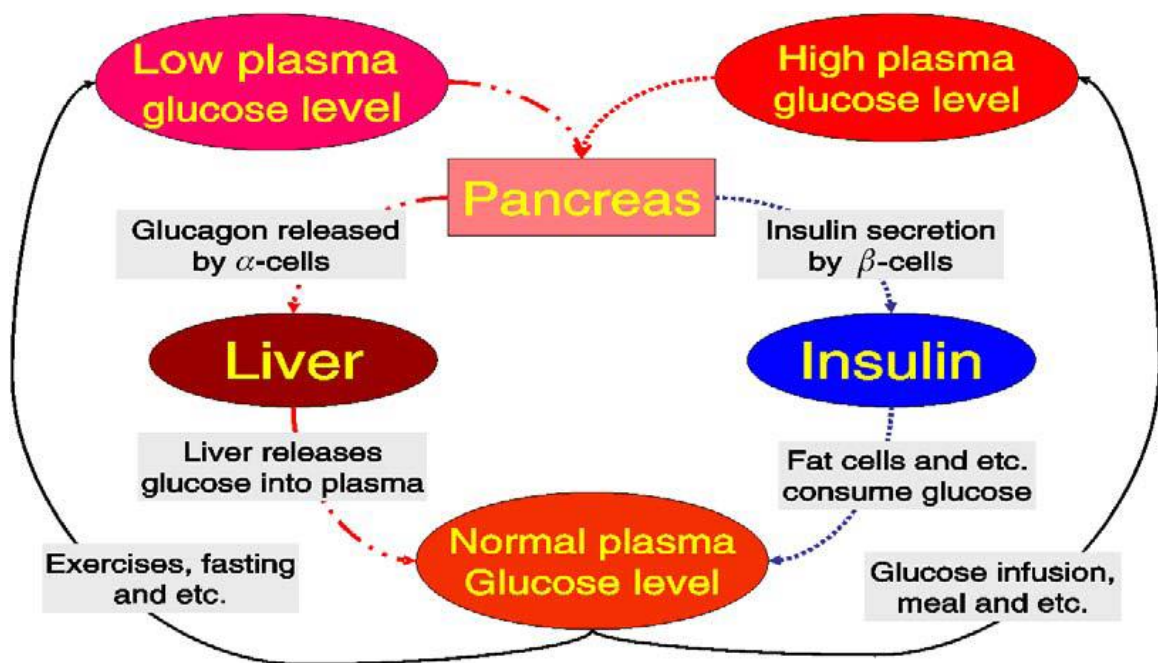


Figure 2.3 Physiological glucose-insulin regulatory system.

2.4.10 Effect of Insulin on Promoting Liver Uptake, Storage and Use of Glucose.

One of the most important of all the effects of insulin is to cause most of the glucose absorbed after a meal to be stored almost immediately in the liver in the form of glycogen. Then, between meals, when food is not available and the blood glucose concentration begins to fall, insulin secretion decreases rapidly and the liver glycogen is split back into glucose, which is released back into the blood to keep the blood glucose concentration from falling too low. When the quantity of glucose entering the liver cells is more than can be stored as glycogen or be used for local hepatocyte metabolism, insulin promotes the conversion of all this excess glucose into fatty acids. These fatty acids are subsequently package as triglyceride in very low density lipoproteins and transported in this form by way of the blood to the adipose tissue and deposited as fat. Insulin also inhibits gluconeogenesis. It does this mainly by decreasing the quantities and activities of the liver enzymes required for gluconeogenesis. However, part of the effect is caused by an action of insulin that decreases the release and in turn the availability of these necessary precursors required for gluconeogenesis.

2.4.11 Lack of Effect of Insulin on Glucose Uptake and Usage by the Brain.

The brain is quite different from most other tissues of the body in that insulin has little or no effect on uptake or use of glucose. Instead, the brain cells are even normally permeable to glucose and can use glucose without the intermediation of insulin. The brain cells are also quite different from most other cells of the body in that they normally use only glucose for energy and can use other energy substrates, such as fats, only with difficulty (Guyton and Hall, 1996). Therefore, it is essential that the blood glucose level be maintained always above a critical level, which is one of the most important functions of the blood glucose control system. When the blood glucose does fall too low, into the range of 20 to 50 mg/dl, symptoms of hypoglycemic shock develop, characterized by progressive nervous irritability that leads to fainting, seizures, and even coma.

2.4.12 Effect of Insulin on Carbohydrate and Metabolism in Other Cells

Insulin increases glucose transport into and glucose usage by most other cells of the body (with the exception of the brain cells as noted) in the same way that it affects glucose transport and usage in the muscle cell. The transport of glucose into adipose cells mainly provides the glycerol portion of the fat molecule. Therefore, in this indirect way, insulin promotes deposition of fat in these cells.

2.5 INSULIN RESISTANCE

This is the failure of exogenously administered insulin to adequately lower blood glucose levels in an individual when compared with others in a defined population (Fasanmade, 1987). The factors leading to the abnormality vary but can be classified into genetic and environmental factors. Normally, when insulin binds to the insulin receptors, the resultant insulin-insulin receptor complex is internalized into the cell by endocytosis and then the insulin is released inside the cell while the receptor is recycled to the surface. This sequence of event could be interrupted at various points to present with insulin resistance (IR). The causes of insulin resistance include:

- i. Abnormal β -cell secretory products
 - a. Abnormal insulin molecule
 - b. incomplete conversion of pro-insulin to insulin
- ii. Circulating insulin antagonists
 - a. Elevated levels of counter regulatory hormones like growth hormone cortisol, glucagon or catecholamines
 - b. Anti-insulin antibodies
 - c. Anti-insulin receptor antibodies
- iii. Target tissue defects
 - a. Insulin receptor defects
 - b. Post-receptor defect.

2.5.1 Determination of Glucose Disappearance Rate as a Quantitative Means of Measuring Insulin Resistance.

The concept of insulin resistance is relatively easy to understand, but determining precisely the insulin resistance is more complicated. The relationship between glucose and insulin is quite complex and involves the interaction of many metabolic and regulatory factors. Normal insulin sensitivity varies widely and is influenced by age, ethnicity and obesity (Castracane and Kauffman, 2003). Simply put, not all persons with impaired insulin sensitivity are necessarily suffering from a disorder, and pregnancy is a perfect example of this (McAuley and Duncan, 2001).

A World Health Organization group recently concluded that the insulin sensitivity (SI) of the lowest 25% of a general population can be considered insulin resistant due to a low value of glucose disappearance rate constant in their respective blood plasma. The European Group of the study of insulin resistance took a more restricted view, defining insulin resistant as the SI of the lowest 10% of a non-obese, non-diabetic, normotensive Caucasian population. Richard

Legro and his associates also used the SI of the lowest 10% of an obese to define insulin resistance.

2.6 TESTS TO MEASURE INSULIN SENSITIVITY

The hyperinsulinemic-euglycemic clamp technique is the most scientifically sound technique for measuring insulin sensitivity, and it is against this standard that all other tests are usually compared. Because this and similar ‘clamp’ techniques are expensive, time consuming and labour intensive, they are not very practical in office setting (Castracane and Kauffman, 2003). To overcome these obstacles, alternative tests have been developed, including the frequently sampled intravenous glucose tolerance test (FSIGTT), short insulin tolerance test (SITT), insulin sensitivity test (IST), and continuous infusion of glucose with model assessment (CIGMA). Unfortunately, all of these methods require intravenous access and multiple venipunctures, making them relatively impractical for office assessment. The oral glucose tolerance test (OGTT) does not require intravenous access but does involve several venipunctures and 2 to 4 hours of patient and technician time. Each of these tests has been shown to correlate reasonably well with dynamic clamp techniques.

2.6.1 Clamp Techniques and Insulin Infusion Test

Hyperinsulinemic-euglycemic clamp: The gold standard for evaluating insulin sensitivity, through “clamp” techniques requires a steady intravenous infusion of insulin to be administered in one arm. The serum glucose level is “clamped” at a normal fasting concentration by administering a variable glucose infusion in the other arm. Numerous blood sampling are then taken to monitor serum glucose so that a steady “fasting” level can be maintained (In theory, the intravenous insulin infusion should completely suppress hepatic glucose production and not interfere with the test’s ability to determine how sensitive target tissues are to the hormones.) The degree of insulin resistance should be inversely proportional to the glucose uptake by target tissues during the procedure. In other words, the less glucose that is taken up by tissues during the procedure, the more insulin resistance a person is (McAuley and Duncan, 2001).

A variation of this technique, the hyperinsulinemic-hyperglycemic clamp provides a better measurement of pancreatic beta cell function but is less physiologic than the euglycemic clamp technique.

Insulin Sensitivity Test (IST): IST involves intravenous infusion of a defined glucose load and a fixed infusion of insulin over approximately 3 hours. Somatostatin may be infused simultaneously to prevent insulin secretion, inhibit hepatic gluconeogenesis and delay

secretion of counter regulatory hormones—particularly glucagon, growth hormone, cortisol and catecholamine. Fewer blood samples are required for this test compared to clamp techniques. The mean plasma glucose concentration over the last 30 minutes of the test reflects insulin sensitivity. Although lengthy, IST is less labour intensive than clamp techniques and the FSIGTT.

Short Insulin Tolerance Test (SITT): A simplified version of IST, SITT measures the decline in serum glucose after an intravenous bolus of regular insulin (0.1-0.5u/kg) is administered. Several insulin and glucose levels are sampled over the following 15 minutes (depending on the protocol used). SITT primarily measures insulin-stimulated uptake of glucose into skeletal muscle. Because the test is so brief, there is very little danger of counter-regulatory hormones interfering with its regulatory action. The glucose disappearance rate constant ‘K’ is determined using the $t_{1/2}$ derived from the slope of the graph of the glucose disappearance rate, the graph being drawn by the line of best fit from the least squares method of regression (Fasanmade, 1987).

Intravenous Glucose Tolerance Test (IVGTT): Is a simple and established experimental procedure in which a challenge bolus of glucose is administered intravenously and blood glucose and insulin concentrations are then frequently sampled (Gaetano and Arino, 2002). This forms the basis for the design of FSIGT.

2.6.2 Minimal Approach Test

“Minimal” models require intravenous or oral administration of glucose only, unlike studies we discussed previously, which require intravenous insulin. This method is less labour intensive than clamp techniques yet still requires as many as 25 blood samples over a 3-hour period, and a computer-assisted mathematical analysis. Several variety of the FSIGTT have been published. One recently published study infused 0.3 g/kg of glucose over 1 minute, followed by tolbutamide 500 mg intravenous at 20 minutes into the glucose infusion. This was calculated by a computer based program. Tolbutamide administration can also be used during FSIGTT to augment endogenous insulin secretion and is particularly useful in women with diabetes (Castracane and Kauffman, 2003).

Continuous Infusion of Glucose with Model Assessment (CIGMA): Like SITT, CIGMA requires fewer venipunctures and is less laborious than clamp techniques. A constant IV glucose infusion is administered, and samples for glucose and insulin are drawn at 50, 55, and 60 minutes. A mathematical model is then used to calculate SI. The results are reasonably compatible with clamp techniques.

Oral Glucose Tolerance Test (OGTT): OGTT, a mainstay in the diagnosis of impaired glucose tolerance (IGT) and diabetes mellitus in pregnant and non-pregnant women may be used to assess insulin sensitivity as well. Because no IV access is needed, OGTT is better suited for assessment of large populations than the other techniques outlined. A modified OGTT that uses a 75 or 100 g glucose load and measures glucose and insulin at various intervals over 4 hours has been used in clinical studies. Like other minimal approaches to diagnosis, OGTT provides information on beta cell secretion and peripheral insulin action, and various mathematical equations have been used to provide SI value (McAuley and Duncan, 2001).

2.7 COMPOSITION OF BLOOD

Blood is a red fluid connective tissue that is pumped throughout the vascular system by the heart. The average 70 kg adult male has a blood volume of about 5 liters. Blood constitutes 6-8% of body weight, the proportion being slightly lower for women and for the obese person (adipose tissue contains little blood), and greater for children (Watson, 2005). Blood consists of a straw-coloured fluid called plasma, which is composed of water and a wide variety of solutes, and the formed elements (blood cells and platelets), which are suspended in the plasma (Figure 2.4) water and solutes are continually being added and removed. Temporary variations in solute concentration occur but, in health, compensatory mechanisms act quickly to maintain plasma concentration within a normal range. An example of the operation of such a mechanism occurs following a meal when blood sugar levels are increased. Within 1-2 hours blood glucose levels are returned to a normal concentration of 70-110mg/dl. Conversely if blood glucose falls, glucose is released into the blood to maintain a normal plasma concentration.

2.8 PROPERTIES OF BLOOD

2.8.1 Viscosity of Blood

The viscosity of blood is approximately 1.8 times the viscosity of water at 37 °C and is related to the protein composition of the plasma. Also, viscosity changes as temperature and blood flow changes. Viscosity increases 2 % for each degree Celsius increased. Low blood flow increases viscosity due to the “cell-to-cell and protein-to-cell adhesive interactions that can cause erythrocytes to adhere to one another” (Hinghofer-Szalkay *et al.*, 1987).

2.8.2 Density of Blood

Blood density is $1,060 \text{ kg/m}^3$ at a 37°C . This measurement shows the entire density of blood as a mixture. Blood is a liquid tissue composed of roughly 55% fluid plasma and 45% cells. The three main types of cells in blood are red blood cells, white blood cells and platelets. 92% of blood plasma is composed of water and the other 8% is composed of proteins, metabolites and ions. The density of blood plasma is approximately 1025 kg/m^3 and the density of blood cells circulating in the blood is approximately 1125 kg/m^3 . Blood plasma and its contents is known as whole blood. The average density of whole blood for a human is about 1060 kg/m^3 . Blood density changes with body posture. Venous blood density is higher when a person is standing than when he is sitting. The following charts show the venous blood densities of 6 subjects as they change body positions during a 10 minute period. Blood density also varies from species to species and between genders within a species (Hinghofer-Szalkay *et al.*, 1987).

2.8.3 Blood Velocity

The velocity of blood in the aorta is determined by a number of factors. The work done by the heart during ventricular contraction is $W = \Delta P V$. With the assumption that the ventricular contraction is instantaneous, and a constant volume of blood undergoes a change in pressure, and then is placed instantly into the aorta and 70 % of the work done by the heart is done by the time the blood reaches its maximum velocity. Also it is assumed that the walls of the aorta are regarded as Hookean "springs". While the aortal walls have very high resilience, their stress versus strain curves is not linear throughout the range of radii which the aorta assumes during pulsatile flow (Richard, 2005). Not all of that energy goes into moving the blood. Some of it is stored as potential energy in the increased blood pressure, some is stored as elastic energy in the walls of the aorta, and some is lost to dissipation as follows;

$$W = K + U_{\text{blood pressure}} + U_{\text{aortal walls}} + E_{\text{dissipation}},$$

where K is the kinetic energy of the blood. The pressure difference ΔP is the difference between the maximum and residual ventricular pressures (the ventricle never empties completely). Assuming a maximum normal (systolic) pressure of 120 mmHg and a residual pressure of 9 mmHg, the pressure difference in the ventricle is 111 mmHg, or $1.5 \times 10^5 \text{ dynes/cm}^2$. The stroke volume V (the amount of blood expelled into the aorta during ventricular contraction) is about 80 cm^3 . This means that the heart does about $1.18 \times 10^7 \text{ ergs}$ of work

during a ventricular contraction. Only about 70% of that work is done before the blood velocity reaches its maximum. So the amount of energy available to move blood at its maximum velocity is 8.29×10^6 ergs. The potential energy of the blood increases as the blood pressure increases from its diastolic to its systolic levels. Assuming a normal diastolic pressure of 80 mmHg, the pressure difference in the blood is 40 mmHg, or 5.3×10^4 dynes / cm². Using 70 % of the stroke volume above, this means that 2.99×10^6 ergs are stored as potential energy in the increased blood pressure. In addition, potential energy is stored in the arterial walls as they expand. If we assume Hookean behavior with a "spring constant" of $k = 1.25 \times 10^6$ dynes / cm and a variation in radius of 0.2 cm in the aorta, 2.5×10^4 ergs are stored in its walls as elastic potential energy. This energy is released as the aorta walls contract and the blood flows into the rest of the system. Note that it is negligible compared to the work done by the heart and the blood pressure potential energy. In order to compute the energy lost to dissipation, Poiseuille's Equation is used to calculate the pressure loss along the aorta, and then compute the energy loss using the stroke volume. The flow rate (assuming 72 beats per minute) is $96 \text{ cm}^3 / \text{s}$. The average radius of the aorta is 1.25 cm, and its length is approximately 30 cm. We find the pressure drop along the aorta to be 120.2 dynes / cm². This means that 9.6×10^3 ergs is lost dissipation. To compute the velocity, simply conserve energy (ignoring elastic energy and dissipation from our above computations): $K = W - U_{\text{blood pressure}}$, or $(1/2) \rho (.7 V) v^2 = 8.29 \times 10^6 - 2.99 \times 10^6$ ergs, where $\rho (.7 V)$ is the mass of the blood moved during the heartbeat, giving $v = 4.25 \times 10^2 \text{ cm} / \text{s}$.

2.8.4 Turbulence

Flow can be categorized into two types: laminar and turbulent. In laminar flow the direction of the flow is parallel to the vessel wall and is basically straight. This type of flow is silent: it does not produce an audible noise of any kind. In turbulent flow the direction of the flow is not parallel to the vessel wall and blood flows in different directions. Turbulent flow can often cause small whirlpools to form in the blood, much like the ones seen in rivers at points of obstruction. This type of flow makes an audible noise which can be heard by a stethoscope. Obviously, flow which is turbulent causes much more resistance in the blood vessel than those laminar flow therefore laminar flow allows for better and easier delivery of blood. There is a considerable turbulence of flow at the branches of large arteries. Also during the rapid phase of ejection by the ventricles turbulent flow occurs at the proximal portions of the aorta and pulmonary artery. However in small vessels blood flow is predominantly laminar (Richard, 2005). Fluid flow in a pipe crosses the threshold from laminar to turbulent flow when a dimensionless parameter called "Reynold's Number" ("Re")

reaches about 2000. It is defined as $Re = \rho l v / \eta$, where v is the velocity of the fluid and l is the characteristic "length" of the pipe. Re is essentially the ratio of the inertial forces (tending to keep the fluid flowing) to the viscous forces (tending to slow the motion due to contact with adjacent layers) experienced by a layer of fluid. Re can also be expressed as the ratio of viscous diffusion time (the time required for effects to diffuse through fluid layers) to eddy advection time (the time required for eddies or vortices to form). Using the value for aortal velocity computed as $v = 4.25 \times 10^2$ cm / s, we see that Re reaches a value of over 28,000 in the aorta (Seed and Wood, 1971). This value is misleading, however, while Re reaches values which might indicate the presence of turbulence in the aorta, it is not clear how long Re remains that large. If it is not that high for an adequate time to form macroscopic eddies, we would not expect to detect the turbulence. The eddy advection time is 0.7 milliseconds, using the formula, $t_a = \text{Sqrt}(\eta \Delta t V / K)$, where Δt is the time duration of a heartbeat, K is kinetic energy of the blood and V is the stroke volume. The eddy length scale, which tells us the size of an eddy which can form in that time, is $l_a = (\eta^3 \Delta t V / \rho^2 K)^{1/4}$, which here comes out to 5.2×10^{-3} cm. These two numbers are characteristic values for our patient, indicating that small eddies are forming and dissipating in very short lengths of time. What then will happen during the much longer time during which blood flows? In normal patients, the velocity reaches its peak and falls in approximately 0.2 s. If, as seems likely from the dependence of t_a and l_a on energy, the length scales as the square root of the time, then the expected aortal eddy size is 0.09 cm. The magnitude of this number indicates that normal flow in the aorta is laminar, but on the verge of turbulence (Seed and Wood, 1971).

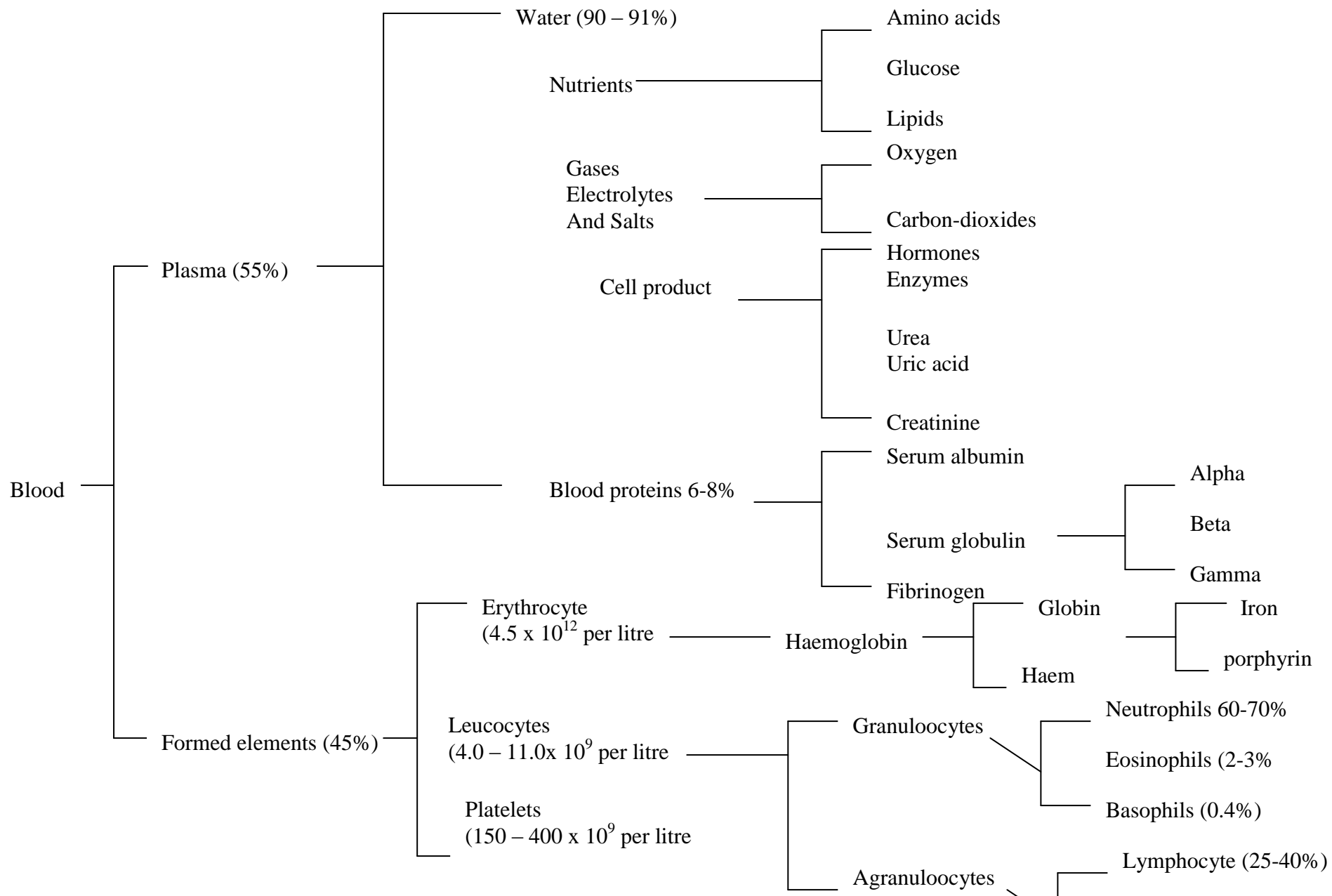


Figure 2.4: Composition of Blood
(Watson, 2005)

2.9 CLASSIFYING MATHEMATICAL MODELS

Many mathematical models can be classified in some of the following ways;

- a. **Linear vs. nonlinear:** Mathematical models are usually composed by variables, which are abstractions of quantities of interest in the described systems, and operators that act on these variables, which can be algebraic operators, functions, differential operators, etc. If all the operators in a mathematical model present linearity, the resulting mathematical model is defined as linear. A model is considered to be nonlinear otherwise.
- b. **Deterministic vs. probabilistic (stochastic):** A deterministic model is one in which every set of variable states is uniquely determined by parameters in the model and by sets of previous states of these variables. Therefore, deterministic models perform the same way for a given set of initial conditions. Conversely, in a stochastic model, randomness is present, and variable states are not described by unique values, but rather by probability distributions.
- c. **Static vs. dynamic:** A static model does not account for the element of time, while a dynamic model does. Dynamic models typically are represented with difference equations or differential equations.
- d. **Lumped parameters vs. distributed parameters:** If the model is homogeneous (consistent state throughout the entire system) the parameters are lumped. If the model is heterogeneous (varying state within the system), then the parameters are distributed. Distributed parameters are typically represented with partial differential equations.

2.9.1 Basis for Mathematical Models

The basis for mathematical models is the fundamental physical and chemical laws, such as the laws of conservation of mass, energy, and momentum (Luyben, 1990). To study dynamics we will use them in their general form with time derivatives included.

(a) *Total continuity equation (mass balance)*

The principle of the conservation of mass when applied to a dynamic system says.

$$\left[\begin{array}{l} \text{Mass flow} \\ \text{int o system} \end{array} \right] - \left[\begin{array}{l} \text{Mass flow} \\ \text{out of system} \end{array} \right] = \left[\begin{array}{l} \text{time rate of change} \\ \text{of mass inside system} \end{array} \right] \quad (2.1)$$

The units of this equation are mass per time. Only one total continuity equation can be written for one system. The right –hand side of equation (2.1) will either be a partial derivative $\partial / \partial t$ or an ordinary derivative d/dt of the mass inside the system with respect to the independent variable t .

(b) Component continuity equations (Component balances)

Unlike mass, chemical components are not conserved if a reaction occurs inside a system, the number of moles of an individual component will increase if it is a product of the reaction or decrease if it is a reactant. Therefore the component continuity equation of the j^{th} chemical species of the system says. The units of this equation are moles of component of j per unit time.

$$\left[\begin{array}{l} \text{Flow of moles of } j^{\text{th}} \\ \text{component int o system} \end{array} \right] - \left[\begin{array}{l} \text{Flow of moles of } j^{\text{th}} \\ \text{component out of system} \end{array} \right] + \left[\begin{array}{l} \text{rate of formation of moles of } j^{\text{th}} \\ \text{component from chemical reaction} \end{array} \right] = \left[\begin{array}{l} \text{time rate of change of moles of } j^{\text{th}} \\ \text{component inside system} \end{array} \right] \quad (2.2)$$

2.9.2 Uses of Mathematical Models

Mathematical models can be useful in all phases of chemical engineering from research and development to plant operations, and even in business and economic studies.

1. **Research and Development:** determining chemical kinetic mechanisms and parameters from laboratory or pilot-plant reaction data; exploring the effects of different operating conditions for optimization and control studies; aiding in scale-up calculations.
2. **Design:** Exploring the sizing and arrangement of processing equipment for dynamic performance; studying the interactions of various parts of the process, particularly when material recycles or heat integration is used; evaluating alternative process and control structures and strategies; simulating start-up, shutdown, and emergency situations and procedures.
3. **Plant Operation:** Troubleshooting control and processing problems; aiding in start-up and operator training; studying the effects of and the requirements for expansion (bottleneck-removal) projects; optimizing plant operation. It is usually much cheaper, safer and faster to conduct the kinds of studies listed above on a mathematical model than experimentally on an operating unit (Luyben, 1990).

2.9.3 Forms of the Mathematical Models

The models are in the form of ordinary differential, partial differential, delay differential and integro-differential equations (Makrogloou and Kuang, 2005). Of all these differential equations, only ordinary differential equation is relevant to this research work and thus will be discussed briefly. By an ordinary differential equation, we shall mean any equation involving a function and derivative of this function (Miller, 1987). Ordinary differential equations contain only functions of a single variable, called the **independent variable** and derivatives with respect to that variable. The order of a differential equation is the order of the highest derivative contained in the equation. Thus.

$$\left(\frac{d^2y}{dx^2} \right)^3 + 4 \frac{dy}{dx} + 5y \frac{dy}{dx} + 6y = 0 \quad (2.3)$$

is an ordinary differential equation of order 2. Here y stands for the unknown function and x is the independent variable.

The broad classifications of equations with which Engineers must contend are: linear and nonlinear equations (Rice and Do, 1995). Much is known about linear equations, and in principle all such equations can be solved by well-known methods. On the other hand, there exist no general solution methods for nonlinear equations. However, a few special types are amenable to solution.

2.10 SOLUTION TECHNIQUES FOR MODELS YIELDING ORDINARY DIFFERENTIAL EQUATIONS (ODE)

The most commonly occurring first order equation in engineering analysis is the linear first order equation (the integrating-factor equation).

$$\frac{dy}{dx} + \alpha(x)y = f(x) \quad (2.4)$$

Which is sometimes called the first order equation with forcing function, $f(x)$ being the forcing function (Rice and Do, 1995). For the general case, given in functional form as equation (2.4), we shall allow the coefficient α and the forcing function f to vary with respect to the independent variable x . it is clear that separation of variables is not possible in the present state. To start the solution of equation (2.4), we put forth the position that there exists an elementary, separable solution.

$$\frac{d}{dx}[I(x)y] = I(x)f(x) \quad (2.5)$$

If such a form existed, then variables are separated and the solution is straight forward by direct integration.

$$y = \frac{I}{I(x)} \int I(x)f(x)dx + \frac{c}{I(x)} \quad (2.6)$$

Where c is an arbitrary constant of integration.

To prove such a solution exists, we must specify the function $I(x)$. To do this, we rearrange equation (2.5) into exactly the same form as equation (2.4)

$$\frac{dy}{dx} + \frac{1}{I(x)} \frac{dI(x)}{dx} y = f(x) \quad (2.7)$$

In order for these two equations to be identical, we must require.

$$\frac{1}{I(x)} \frac{dI(x)}{dx} = \alpha(x) \quad (2.8)$$

or, within a constant of integration.

$$I(x) = \exp\left(\int \alpha(x) dx\right) \quad (2.9)$$

Where $I(x)$ is called the **integrating factor**. This is the necessary and sufficient condition for the general solution, equation (2.6), to exist.

Other solution techniques but not relevant to this work include:

- Exact solutions
- Transformation of equations to Homogenous functions
- Transformation of equations into Bernouli's and Riccati's form to be solved using the integrating factor method and etc.

2.10.1 Laplace Transformation as a Special Case of Solving Linear ODE.

The use of Laplace transformations yields some very useful simplifications in notation and computation. Laplace-transforming the linear ordinary differential equations describing our processes in terms of the independent variable t convert them into algebraic equations in the Laplace transform variables. This provides a very convenient representation of system dynamics (Luyben, 1990).

After transforming equations into the Laplace domain and solving for output variables as functions of s , we sometimes want to transform back into the times domain. This operation is called **inversion** or **inverse Laplace transformation**.

2.11 SOLUTION TECHNIQUES FOR PDE'S

Partial Differential Equations (PDE) fall into several categories and some methods may only be applied to certain types of equations. The three classifications are hyperbolic, elliptic and parabolic. As the Blood Flow Equations fall into the classification of

hyperbolic PDE's, the main focus will be on methods suitable for solving hyperbolic equations.

2.11.1 Analytical Methods

Prior to the development of computers and applications to computational fluid dynamics (CFD) analytical techniques had to be used to solve PDE's. However their application to anything but the simplest of problems could be quite cumbersome and require extensive hand computation. One particular method suited to solving problems based on conservation laws is known as the method of characteristics. This technique is still used today, most commonly as a semi-graphical method and also as a means to generate alternative differential equations. The underlying principles of the method of characteristics form the basis for many numerical schemes.

2.11.2 The Method of Characteristics

The method of characteristics can only be applied to hyperbolic PDE's and involves defining the characteristics along which disturbances propagate, Cunge and Verwey (1980). Characteristics can be thought of as lines in the space-time plane, along which (by definition) certain properties are constant. To illustrate the basis of the method, consider a first order PDE of the form

$$u_t + a(x,t)u_x = 0 \quad (2.10)$$

with the initial data $u(x,0) = u_0(x)$. By the chain rule

$$\frac{du}{dt} = u_t + \frac{dx}{dt}u_x \quad (2.11)$$

and rearrangement gives

$$u_t = \frac{du}{dt} - \frac{dx}{dt}u_x \quad (2.12)$$

Substituting equation (2.12) for u_t into equation (2.11) then yields

$$\frac{du}{dt} + \left(a(x,t) - \frac{dx}{dt} \right) u_x = 0 \quad (2.13)$$

From (2.13) it can be seen that $du/dt = 0$ along the lines defined by $dx/dt = a(x,t)$, which implies that the solution u is constant along these lines known as the characteristics. In principle if one can define a set of characteristic lines then it is possible to know the solution at all times (providing the lines do not intercept) just from the initial and boundary conditions of the problem. Mathematically this is equivalent to saying

$$u(x,t) = u\left(x - \int_0^t a(x,t) dt, 0\right). \quad (2.14)$$

If the method is applied over a finite region, then it is necessary to specify the values along any boundary where the characteristics enter the region.

The same principles can be applied to the case

$$u_t + a(u)u_x = 0. \quad (2.15)$$

where if $f'(u) = a(u)$ then

$$u_t + f(u)_x = 0 \quad (2.16)$$

which is a scalar conservation law. Now the characteristics are given by

$$\frac{dx}{dt} = a(u) \quad (2.17)$$

If u is constant along the characteristics so too is a , and the characteristics are straight lines with values determined by the initial conditions. From ordinary differential equation (ODE) theory it can be shown that for continuous u the characteristic lines do not cross. However, hyperbolic PDE's admit discontinuous solutions, and for a general non-linear conservation law with arbitrary initial conditions, the characteristics will cross in finite time and a discontinuity or shock will form. In this instance it is no longer possible to trace back along the characteristic paths to find the solution. If a discontinuity does form, then if u has constant values in either side of the shock then it is possible to calculate a speed s with which the shock moves by applying conservation principles over the region, Le Veque (1992) and Sweby (1993). This leads to the Rankine-Hugoniot jump condition which relates the shock speed to the left and right values such that.

$$s = \frac{f_R - f_L}{u_R - u_L} \quad (2.18)$$

where the subscripts **L** and **R** denote the values to the left and the right of the shock respectively. From the formula the shock position (x_s) can be deduced as $s = dx_s/dt$

Similarly the theory of characteristics can be extended to linear systems of equations of the form.

$$U_t + AU_x = 0 \quad (2.19)$$

Where **U** is a vector, **A** is a constant matrix and $F(U) = AU$. The system can then be decoupled by diagonalising **A** to form a series of scalar equations, each of which will have its own equation to describe the characteristics. For a system of order **n**, the resulting decoupled equations can be rewritten as

$$(v_k)_t + \lambda(v_k)_x = 0 \quad k = 1, 2, \dots, n \quad (2.20)$$

Where v is defined as $v = R^{-1}U$ using **R**, the matrix of the right eigenvectors of **A** and λ_k are the eigenvalues. The characteristics are then represented by

$$\frac{dx}{dt} = \lambda_k \quad (2.21)$$

In terms of the Rankine-Hugoniot relationship, the jump condition becomes

$$A(U_L - U_R) = s(U_L - U_R)$$

Where $U_L - U_R$ then corresponds to the eigenvectors of **A** and s relate to the eigenvalues. In the case where **A** is a non-constant matrix that depends upon **U**, the system is non-linear and so it is not possible to decouple the equations as in the linear case. However, it may still be possible to apply the technique to yield expressions for the characteristics lines for some simplified problems, though in general this will not be the case. The Rankine-Hugoniot relationships also hold for non-linear problems. But again in general it will not be possible to obtain a closed form for the solution.

2.11.3 Numerical Methods

For most problems of practical interest it is not possible to find exact solutions by using analytical techniques such as the method of characteristics. As a result, this has led to the development of numerical methods whereby the continuous problem, i.e. the governing equations, is transformed into a discrete form which then results in a series of algebraic equations which can be solved on a computer. The solution to the discrete problem represents an approximation to the solution of the continuous problems and various

concepts have been developed in an attempt to quantify how well the calculated numerical solutions compare to the true solutions.

2.11.3.1 General Classification of Numerical Methods.

Many techniques are available for numerical simulation work, and a number of broad headings exist to describe how each particular method (or scheme) works. The four most popular types of method for general fluid flow problems are

1. Finite Difference Methods (FDM)
2. Finite Element Methods (FEM)
3. Spectral Methods
4. Finite Volume Methods (FVM)

There is a certain amount of overlap between these classifications and under certain circumstances a particular scheme may fall into more than one category so there is no strict definition as how to identify a method. The following general descriptions are taken from Hirsch (1998) and Versteeg and Malalasekera (1995).

Generally speaking a finite difference method represents the problem through a series of values at particular points or nodes. Expressions for the unknown are derived via replacing the derivative terms in the model equations with truncated Taylor series expansions. The earliest numerical schemes are based upon finite difference construction and are conceptually and intuitively one of the easier methods to implement. However, fundamentally such techniques require a high degree of regularity within the mesh and so this limits their application to complex problems.

The basis of the finite element methods is to divide the domain into elements such as triangles or quadrilaterals and to place within each element nodes at which the numerical solution is determined. The solution at any position is then represented by a series expansion of the nodal values within the local vicinity of that position. The nodal contributions are multiplied by basic functions (also known as shape, interpolation or trial function), and the particular way in which the basic functions are defined determines the choice of variant of the finite element method. Spectral methods can be considered as a subset of the finite element method in which the basic functions are definite globally as opposed to the more common approach whereby the basic functions are local and so is zero outside the neighborhood of the associated node. The original finite element method

was developed within the field of stress analysis and this is reflected within the construction and nomenclature of the approach.

The finite volume method is based upon forming discrimination from an integral form of the model equations, and entails subdividing the domain into a number of finite volumes. Within each volumes the integral relationship are applied locally and so exact conservation within each cell is achieved. The resulting expressions for the unknown often appear similar to finite difference approximations and depending upon the particular method chosen, may be considered as a special case of either the finite difference or finite element techniques. With the emphasis of most fluid modeling problems being based upon conservation principles, the finite volume methods has become the more popular approach for general fluid flow problems.

2.11.3.2 Accuracy, Consistency, Stability, Convergence and Well Posedness.

In order to quantify how well a particular numerical technique performs in generating a solution to a problem, there are four fundamental criteria that can be applied to compare and contrast different methods. The four concepts are accuracy, consistency, stability and convergence. In theory these criteria apply to any form of numerical method though they are easily formulated for finite difference scheme.

Accuracy is a measure of how well the discrete solutions represent the exact solution of the problems. Two quantities exist to measure this. The local or truncation error, which measures how well the difference equations match the differential equations and the global error which reflects the overall error in the solution and in reality, is not possible to find unless the exact solution is known. An expression for the truncation error can be obtained by substituting the known exact solution of the problem into the discretisation leaving a remainder which is then a measure of the error. Alternatively, the exact solution to the discretised problem could be substituted into the differential equation and the remainder obtained. For example for a PDE this would lead to an expression of the form $\tau = O(\Delta t^q, \Delta x^p) = 0$ where τ is the truncation error and Δt and Δx are the time and spatial steps (assuming a regular grid). From this, the method is said to be q^{th} order in time and p^{th} order in space, and generally this is referred to as the level of accuracy of the scheme, Hirsch (1998). It is natural to assume that by increasing the grid resolution then any

error will be reduced and this leads to the definition of consistency. Mathematically, for a method to be consistent then the truncation error must decrease as the step size is reduced which is the case when $q, p \geq 1$, which is equivalent to saying that as $\Delta t, \Delta x$ tend to zero then the discretised equations should tend towards the differential equation. For a scheme to be of practical use, it must be consistent.

Formally if a scheme is said to be stable then any error in the solution will remain bounded. In practice if an unstable method is used then the solution will tend towards infinity. Most methods have stability limits which place restrictions on the size of the grid spacing (i.e. $\Delta x, \Delta t$) that can be used, usually in terms of a limit on the Courant-Friedrichs-lewy (CFL) number. Physically a stable method can be interpreted to be one where the grid points used in the calculation enclose the characteristic lines or domain of dependence. A number of methods are available for obtaining expressions for the stability conditions, and the appropriate choice depend on the actual problem, Smith (1985).

Another requirement is that the numerical scheme should be convergent, which by definition means that the numerical solution should approach the exact solution as the grid spacing is reduced to zero. This is coupled with the global error. However, it is usually not possible to prove the convergence of a particular scheme to a specific problem. Instead use is made of Lax's Equivalence theorem which states that for a well posed initial value problem (IVP) and a consistent method, stability implies convergence, in the case of a linear problem. For non-linear equations, stability and consistency are necessary but not sufficient condition for convergence.

These criteria dictate whether a particular numerical scheme is suited to solving a particular problem. There is another condition, which has to be satisfied in order to produce a valid solution and this relates to the actual problem and is the issue of well posedness. In order to generate a numerical solution, the problem being considered must be well posed. For this to be the case then the following condition must hold

- a) a solution must exist
- b) the solution should be unique
- c) the solution should depend linearly on the data in some way.

The last condition can be translated to mean that the solution should not be sensitive to small changes in the initial/boundary data of the problem. If a problem is not well posed,

then a valid numerical solution cannot be generated and any numerical treatment will either fail or produce poor results. One easy way to produce an ill posed problem is to apply inappropriate boundary conditions, for example by trying to enforce values of the quantities being modeled on the characteristics leaving the computational domain. If the initial data is not fully specified, then this also presents an ill posed problem as there will be no unique solution, Versteeg and Malalasekera (1995).

2.11.3.3 Grid Generation and Explicit/Implicit Formulations

An important factor in applying numerical techniques not yet mentioned here is the question of grid generation, which is an area of research in its own right. Early efforts focused on using regular grids, whereby all the cells or elements were of the same size. Although this has advantages in terms of numbering the cells and forming the discrete equations, for problems requiring a fine resolution having small cells everywhere leads to unnecessary computation and is computationally expensive. In addition, for 2-d and 3-d problems, fitting a regular grid to complex geometries can often lead to problems. To

overcome the difficulties created in implementing regular grids attention has moved towards irregular grids where the cell sizes vary within the domain. Furthermore unstructured (as opposed to structured) gridding has been introduced, leading to the ability to map any region. However, the resulting meshes generally have no apparent structure and so increase the level of complexity of generating suitable computer code. The predominant reason for using irregular gridding is the ability to concentrate the cells in areas where sharp gradients occur, and so a high level of accuracy can be maintained throughout the region without the need to us a fine grid everywhere. If such a grid is generated at the outset of a problem, it may be that as the simulation progresses, the initial choice is no longer the most suitable, and so this has led to the idea of adaptively whereby the grid evolves during the simulation, in a manner determined by the numerical solution, Yee (1987).

Another distinction that can be drawn between different methods is whether they are explicit or implicit. For example, taking the linear advection equation

$$u_t + au_x = 0 \quad a = \text{constant} \quad (2.22)$$

then if the solution is to be advanced to time level $n+1$, the spatial derivative may be approximated either in terms of the known value at time level n or the unknown quantities at level $n+1$. If an approximation for the spatial derivative is approximated at time level n then that corresponds to an explicit method, whereas using level $n + 1$ represents an implicit formulation. Figure 2.5 shows a rectangular net of mesh for finite difference of derivatives. Both explicit and implicit schemes have there relative merits. Explicit methods are generally simpler in terms of the resulting algebraic equations as implicit schemes usually require a matrix inversion which is more costly. However, most implicit scheme are not restricted by the CFL stability constraints placed upon the explicit counterparts, and so allow the use of much larger time steps.

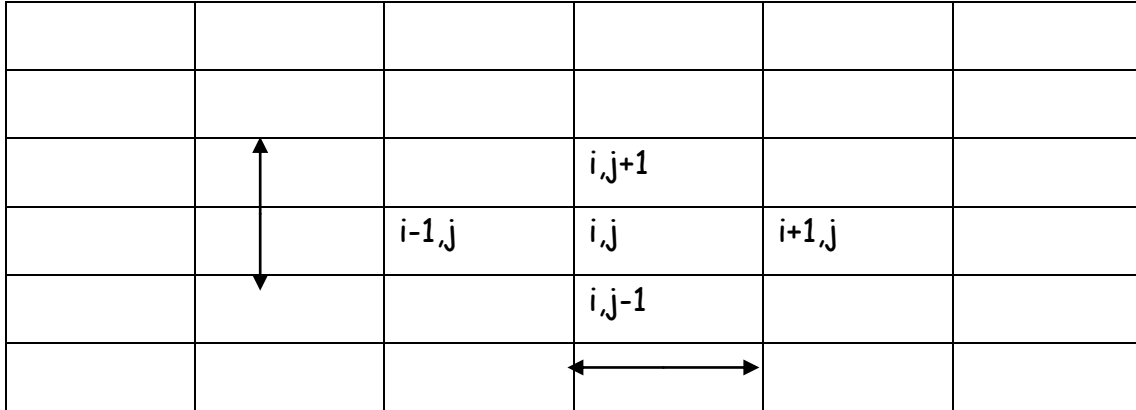


Figure 2.5. Rectangular net of mesh for finite difference of derivatives

2.11.3.4 Numerical Methods for Conservation Laws

This work is mainly concerned with modelling conservation laws which may be exported either in differential or integral form, i.e for a 1-d system in Cartesian coordinates

$$U_t + F_x = R \quad (2.23)$$

or

$$\oint (Udx - Fdt) = \int R d\Omega \quad (2.24)$$

where the integral form is more general than the differential form as it is valid for discontinuous solutions. In particular, the focus of the study is to investigate ways to improve (in terms of accuracy and reduced run times) the explicit scheme currently popular within the hydraulics community, which are predominantly formulated within the

finite-difference/finite-volume framework and make use of Riemann based solutions. This section now goes on to identify some of the desirable/required properties of scheme suitable for solving conservation laws and discusses the concept of finite difference and finite volume scheme in more detail. Some of the ‘classical’ schemes are then introduced together with some subsequent advances made in their application. A description of the Godunov (1959) method is made as this formed the starting point of the finite volume approach and Riemann based schemes.

2.11.3.5 Desirable Properties of Numerical Methods for Conservation Laws

Aside from the requirements of ensuring that any chosen scheme be consistent, stable and convergent, a number of additional criteria can be defined for identifying methods that are suitable for modeling conservation laws. The fact that most conservation laws are non-linear introduces additional problems not apparent with linear equations and also complicates the mathematical analysis. In particular non-linear equations often give rise to discontinuous solutions. Some techniques experience difficulties in solving discontinuous flows and spurious oscillations can appear in the numerical solution. There is also the issue of generating the right solution, as discontinuous solution correspond to weak solutions of the differential equation, meaning that there may be more than one correct (in terms of satisfying the differential equation) solution. Under such circumstances additional information is required to isolate the correct result.

There exist certain criteria for assessing if a particular scheme is suited to solving conservation law problems and these give rise to conservative methods Le Veque (1992). If a method is conservative then when it is applied to a conservation law (expressed in conservation form). Then the sum of contributions from the discrete representation of the flux terms should cancel everywhere except at the boundaries. Apart from ensuring that the discrete system is conservative, then if the solution is discontinuous, using a conservative method also means that the numerical solution will correspond to a weak solution of the equations, and this is the basis of a theorem by Lax and Wendroff. However, this does not guarantee that the scheme will produce the physically correct weak solution for a given problem. In the case where more than one weak solution exists, the correct solution is determined via an entropy condition, so named after its origin in gas dynamics. Effectively

this condition can be translated in terms of the characteristics which say that the characteristics cannot emerge from a physically valid shock.

A strategy which can enable the use of some scheme which cannot resolve discontinuities correctly is to use a shock tracking approach. The idea then is to use the chosen scheme throughout most of the region and to isolate the position of any discontinuities which are then treated separately. Conversely shock capturing methods are ones in which no account is made of where any discontinuities occur and the same scheme is employed throughout the domain and any shock formed occur at the correct location.

Another concern connected with discontinuous solution is the generation of oscillations in regions containing strong gradients. Such oscillations are a problem as they can lead to non-physical negative quantities, and specific criteria have been developed to assess whether or not particular schemes will give rise to oscillation. Methods which satisfy these conditions are known as Total Variation Diminishing (TVD) scheme Le Veque (1992).

The manner in which the flux term is discretised can either be described as upwinded or centralized. The distinction between the two lies in which cells are used to approximate the flux at a particular point. Upwind methods take account of the flow direction, and so use values corresponding to the direction from which the characteristics originate. Central schemes use a symmetric discretisation and so make no allowances for the characteristic direction. For convective dominated flows, taking an upwind approach is generally considered to be the better option as the flow direction is considered.

2.11.4 Finite Difference Methods (FDM)

Finite difference methods were the first techniques to be developed for approximating ordinary differential equations, and it is from such applications that the theories regarding their properties have been generated.

Finite difference methods are based on performing Taylor series expansion and substituting the truncated expressions into the differential equation. The idea is to approximate the differentials by differences in the solution at various points, Hirsch (1988). By definition

$$u_x \equiv \left(\frac{\partial u}{\partial x} \right) = \lim_{\Delta x \rightarrow 0} \frac{u(x + \Delta x) - u(x)}{\Delta x} \quad 2.25$$

When Δx is small this formula can be used as an approximation for the derivative of u at x .
From Taylor series

$$u(x + \Delta x) = u(x) + \Delta x u_x(x) + \frac{\Delta x^2}{2} u_{xx}(x) + \dots \quad (2.26)$$

and so by rearrangement

$$\frac{u(x + \Delta x) - u(x)}{\Delta x} = u(x) + \Delta x u_x(x) + \frac{\Delta x^2}{2} u_{xx}(x) + \dots \quad (2.27)$$

If Δx is small the successive terms in the expansion will decrease and so it is possible to write

$$u_x(x) = \frac{u(x + \Delta x) - u(x)}{\Delta x} + O(\Delta x) \quad (2.28)$$

From equation (2.28), the leading term of the error in approximating u_x by the right hand side is of order Δx and so this represents a first order approximation. It is possible to define order difference formula to approximate derivatives and these may have different order of accuracy.

The above analysis deals with the continuous solution however, the objective is to calculate u at a set of discrete point on the mesh, and this is the numerical solution. Let the mesh points be denoted by x_i where $i = 1, 2, 3, \dots, N$ and the region has been discretised into N equally sized elements of length Δx . Then the numerical solution u_i , can be thought of as point value where $u_i = u(i\Delta x)$. Following this notation, there are three common ways to approximate the first derivative of u with respect to x ,

(i) Forward difference

$$(u_x)_i = \frac{u_{i+1} - u_i}{\Delta x} + O(\Delta x) \quad (2.29)$$

(ii) Backward difference

$$(u_x)_i = \frac{u_i - u_{i-1}}{\Delta x} + O(\Delta x) \quad (2.30)$$

(iii) Central difference

$$(u_x)_i = \frac{u_{i+1} - u_{i-1}}{2\Delta x} + O(\Delta x^2) \quad (2.31)$$

As can be seen, both the forward and backward differences are first order approximations whereas the central difference is second order, as can be shown by Taylor series analysis.

These formulas have different merits and the best choice depends on the problem being modeled. In the case of ODE's, many other difference formulas can be derived and standard techniques are available for doing so. However for PDE's, most scheme are based upon using standard forward backward and central difference formula.

2.11.4.1 Classical Finite Difference Methods for Conservation Laws

The classical numerical methods used to solve partial differential equation are based upon limit difference construction and can be best illustrated through means of an example, in this case via the linear advection equation,

$$u_t + (au)_x = 0 \quad (2.32)$$

where $f = au$ and a is constant. This equation often used as a test problem to validate methods for modeling transport dominated flows, as the analytical solution at a time t is given by the translation of the initial data by a distance, at .

The general distinctions that can be made between different schemes refer to the way in which the terms in the differential equation are approximated, and this in turn corresponds to the temporal and spatial levels of the value within the difference equation. The way in which most schemes are described is to say whether they are explicit or implicit, upwind or centralised, TVD or not, and to specify the stability constraints and level of accuracy of the method. Some schemes are only applied to the spatial derivatives (or flux terms) and require a separate treatment of the temporal derivatives, whilst others combine both the time and space integrations, Le Veque (1992).

One of the simplest schemes to implement for the linear advection equation is the first order upwind scheme. As the name suggest this method is first order in space and time and is based on using an upwind difference formula. For eqn. 2.32 this scheme can be written as

$$u_i^{n+1} = u_i^n - \nu \begin{cases} u_{i+1}^n - u_i^n & \dots \text{if } a < 0 \\ u_i^n - u_{i-1}^n & \dots \text{if } a > 0 \end{cases} \quad (2.33)$$

where $\nu = a\Delta t/\Delta x$ and is the Courant number or CFL value. Although this method has the advantages of being both upwinded and TVD, it is only first order accurate and so heavily smears discontinuous profiles.

To obtain a scheme with a higher formal order of accuracy, the central difference formula can be used. For example, the Leapfrog scheme uses central differencing for both the time and space derivatives to give

$$u_i^{n+1} = u_i^{n-1} - \nu(u_i^{n+1} - u_i^{n-1}) \quad (2.34)$$

One of the problems with this method is that the update involves three time levels which are both cumbersome in terms of memory storage and also in starting the simulation. In practice, methods involving more than two time levels in the update are now used to solve time dependent conservation laws problems. If the time derivative in the leapfrog method is replaced with the one sided difference

$$u_t \approx \frac{u_i^{n+1} - u_i^n}{\Delta t} \quad (2.35)$$

then the resulting scheme is unstable. If u_i^n in equation (2.35) is replaced by the average $(u_{i+1}^n - u_{i-1}^n)/2$ then the Lax-Friedrichs scheme is obtained

$$u_i^{n+1} = \frac{1}{2}(u_{i+1}^n + u_{i-1}^n) - \frac{1}{2}(u_{i+1}^n - u_{i-1}^n) \quad (2.36)$$

for which the solution is only first in space and time. By returning to Taylor series and the expansion for u_i^{n+1}

$$u_i^{n+1} = u_i^n - a\Delta t u_t \dot{:}_i^n + \frac{a^2 \Delta t^2}{2} u_{tt} \ddot{:}_i^n + O(\Delta t^3) \quad (2.37)$$

and noting that from the original conservation law

$$u_t = -au_x \quad \text{and} \quad u_{tt} = -a^2 u_{xx} \quad (2.38)$$

the Lax-Wendroff scheme can be obtained by replacing the temporal derivatives in equation (2.37) with spatial derivatives, which are then substituted for central differences to give

$$u_i^{n+1} = u_i^n - \frac{1}{2}\nu(u_{i+1}^n + u_{i-1}^n) - \frac{1}{2}\nu^2(u_{i+1}^n - 2u_i^n + u_{i-1}^n) \quad (2.39)$$

the resulting scheme is second order in both space and time and is prone to oscillations in areas upstream of regions containing sharp gradients, Hirsch (1988). Another scheme which is second order in space and time but based upon using a one-sided difference formula in equation (2.37) is the Warming and Beam (second order upwind) method. With this method oscillation due to discontinuities occur after the shocks and the resulting discretisation (for $a > 0$) is

$$u_i^{n+1} = u_i^n - \frac{1}{2}\nu(3u_i^n - 4u_{i-1}^n + u_{i-2}^n) - \frac{1}{2}\nu^2(u_i^n - 2u_{-1i}^n + u_{i-2}^n) \quad (2.40)$$

By averaging the Lax-Wendroff and Warming and Beam methods, the Fromm scheme is obtained which is also second order accurate. The resulting scheme still suffers from oscillations which occur both in front of and behind any shocks, but the magnitude of the oscillations is reduced (as compared with the Lax-Wendroff and Warming and Beam schemes).

All of the schemes listed so far are explicit. Corresponding implicit versions of these explicit difference methods can be obtained by evaluating the right hand sides of the update formulas at level $n + 1$. However, in general a scheme produced in this way may have different properties from its explicit counterpart. As explicit schemes are more practical to implement, most of the popular finite difference methods are constructed in this manner, Le Veque (1992).

The simplest implicit scheme, known as the Backward Euler scheme can be written as

$$u_i^{n+1} = u_i^n - \frac{1}{2}\nu(u_{i+1}^{n+1} + u_{i-1}^{n+1}) \quad (2.41)$$

for the linear advection equation and is second order in space and first order in time. However this method leads to a tridiagonal matrix system, which may be easy to solve in the linear case (e.g by using the Thomas algorithm) but will require the use of an iterative method for non-linear problems.

Another implicit methods is the Box scheme

$$\left(\frac{u_{i+1}^{n+1} - u_{i+1}^n}{2\Delta t} + \frac{u_i^{n+1} - u_i^n}{2\Delta t} \right) + a \left(\frac{u_{i+1}^{n+1} - u_i^{n+1}}{2\Delta x} + \frac{u_{i+1}^n - u_i^n}{2\Delta x} \right) = 0 \quad (2.42)$$

which is of particular important to computational hydraulics as it forms the basis of the Preissmann scheme which for a homogeneous conservation law is written as

$$\frac{U_{i+1}^{n+1} - U_i^{n+1}}{2\Delta t} + \frac{U_{i+1}^n - U_i^n}{2\Delta t} + \frac{0F_{i+1}^{n+1} + (1-0)F_{i+1}^n}{\Delta x} - \frac{0F_i^{n+1} + (1-0)F_i^n}{\Delta x} = 0 \quad (2.43)$$

where $0.5 \leq \Theta \leq 1$.

2.11.4.2 Extensions of Classical Methods – TVD Scheme and Systems of Equations
All the methods introduced so far in this section have been constant coefficient schemes as were commonly used before the 1980's. One particular consequence of using constant

coefficient scheme is Godunov's (1959) theorem, which states that it is not possible to construct a constant coefficient scheme that is at least second order and will not give rise to spurious oscillations. As most conservation laws are non-linear and admit discontinuous solutions, an effort was made to overcome this difficulty by developing new higher order non-linear scheme which would satisfy the TVD conditions and so not generate oscillations around shocks. This led to the generation of high resolution TVD methods. TVD scheme can be subdivided into two classifications, Sweby (1993).

1. Post-processing scheme: These include Flux Corrected Transport (FCT) and flux limited scheme whereby the solution is obtained by a modified first order scheme.
2. Pre-processing scheme. The data is altered before application of the numerical method.

2.11.5 Finite Volume Methods (FVM)

The fundamental difference between these methods and FDM's is that in FDM's the differential form of the equations are discretised, whereas for FVM's the discretisation is performed on an integral formulation of the equations. The resulting discretisation often resembles those obtained through the use of FDM's and in addition the FVM may be thought of as a subdivision of the FEM, Hirsch (1988). The basis of the finite volume method is to construct an integral form of the governing equations which is valid for any arbitrary closed volume. On a Cartesian mesh, the conservation law can then be represented by

$$\oint (Udx - Fdt) = \int_{\Omega} R d\Omega \quad (2.44)$$

The resulting expression is then applied locally within each cell or finite volume, ensuring that exact conservation of the conserved variable is maintained.

Within this framework, the discrete values of u are considered to be cell average values represented by

$$U_i^n = \frac{1}{\Delta x} \int_{x_{i-1/2}}^{x_{i+1/2}} U(x, t_n) dx \quad (2.45)$$

where $x_{i\pm 1/2}$ correspond to the cell boundaries. Generally the numerical solution is considered to be constant within each cell; however some methods assume other distributions for which the cell average is defined by equation (2.45). By treating the numerical flux function as a time average value of the physical flux function, i.e by defining the numerical flux as

$$F_{i+1/2} = \frac{1}{\Delta t} \int F[U(x_{i+1/2}, t)] dt \quad (2.46)$$

the resulting discretisation of the integral formulation of the homogeneous form of the conservation law can be written as

$$U_i^{n+1} = U_i^n + \frac{\Delta t}{\Delta x} [F_{i-1/2} - F_{i+1/2}] \quad (2.47)$$

which then resembles a finite difference scheme. As with finite difference methods, the way in which $F_{i\pm 1/2}$ is approximated correlates to a particular choice of numerical scheme.

One way to generate the numerical flux is to solve a series of Riemann problems, and this will be discussed later.

2.11.5.1 Godunov Type Schemes and the Finite Volume Framework

One of the first attempts to develop an upwind scheme suitable for solving systems of conservation laws was by Courant Isaacson and Rees (CIR). The CIR method was based upon tracing the characteristics one time level to the next and employed the characteristic form of the equations. Originally this technique was considered for the Euler equations, however as the conservation was not based on the conservation form of the equations, the method was not well suited for solving problems containing discontinuities. Subsequently, in 1959 Godunov published a new technique which differed from previous schemes in that it assumed the numerical solution was constant within each cell, instead of considering nodal values. The basis of the method was to solve series of Riemann problems between each of the cell interfaces and this led to an expression for the numerical flux. The method was explicit and required that the time step was limited in such a way that neighbouring Riemann problems would not interact. The method is introduced here because it was the starting point for the Riemann based schemes. The first stage of the Godunov (1959)

method is to assign the discrete cell average values which are represented by the integral relationship

$$U_i^n = \frac{1}{\Delta x} \int_{x_{i-1/2}}^{x_{i+1/2}} U(x, t_n) dx \quad (2.48)$$

where $x_{i\pm 1/2}$ are the cell boundaries and $U(x, t_n)$ is the known solution at time t_n which is constant within each cell, Le Veque (1992) and Toro (1997). The result is that at each interface, the discrete representation of the data corresponds to the initial data of a Riemann problem. Having calculated the exact solution of the Riemann problem over the time interval $[t_n, t_{n+1}]$, the solution at the next time level is then given by averaging the exact solution of the Riemann problem over each cell such that

$$\bar{U}_i^{n+1} = \frac{1}{\Delta x} \int_{x_{i-1/2}}^{x_{i+1/2}} \bar{U}^n(x, t_{n+1}) dx \quad (2.49)$$

where $\bar{U}^n(x, t_{n+1})$ is taken to be exact solution of the Riemann problem at time t_{n+1} . As \bar{U}^n represents as exact solution to the conservation law, then applying the integral form of the conservation law within a particular cell gives

$$\int_{x_{i-1/2}}^{x_{i+1/2}} \bar{U}^n(x, t_{n+1}) dx = \int_{x_{i-1/2}}^{x_{i+1/2}} \bar{U}^n(x, t_n) dx + \int_{t_n}^{t_{n+1}} F\left(\bar{U}^n(x_{i-1/2}, t)\right) dt - \int_{t_n}^{t_{n+1}} F\left(\bar{U}^n(x_{i+1/2}, t)\right) dt \quad (2.50)$$

From equation (2.49) and using $\bar{U}^n(x, t_n) \equiv U_i^n$ then the update for cell i becomes

$$U_i^{n+1} = U_i^n - \lambda [F(U_i^n, U_{i+1}^n) - F(U_{i-1}^n, U_i^n)] \quad (2.51)$$

when the numerical flux is defined as

$$F(U_i^n, U_i^{n+1}) = \frac{1}{\Delta t} \int_{t_n}^{t_{n+1}} F\left(\bar{U}^n(x_{i+1/2}, t)\right) dt \quad (2.52)$$

The problem then reduces to determining \bar{U}^n over the time interval $[t_n, t_{n+1}]$ at the point $x_{i+1/2}$ which by virtue of the Riemann problem is constant (assuming that the neighbouring Riemann problems do not interact). Denoting this value as $U^*(U_i^n, U_i^{n+1})$ then the first becomes

$$F(U_i^n, U_i^{n+1}) = F(U^*(U_i^n, U_i^{n+1})) \quad (2.53)$$

and so the update can then be written as

$$U_i^{n+1} = U_i^n - \lambda [F(U^*(U_i^n, U_{i+1}^n)) - F(U^*(U_{-1i}^n, U_i^n))] \quad (2.54)$$

2.11.6 Method of Weighted Residuals (MWR)

The method of weighted residuals is another general method of obtaining approximate solutions to partial differential equations, PDE's. The unknown solutions expanded into a set of specified trial functions with adjustable constants (or functions), which are chosen to give the best solution to the differential equation (Finlayson 1972, 1980).

The method of weighted residuals comprises several basic techniques, all of which have proved to be quite powerful. They have been shown by Finlayson (1972, 1980) and Villadsen and Michelsen (1978) to be superior to finite difference schemes for the solution of complex differential equation systems, by being more accurate or by requiring less computation time to generate or both. Unlike the method of variation principles which is not generally applicable and which requires a good deal of mathematical manipulations, the MWR is general.

2.11.6.1 The Collocation Method

Trial function expansion is a proven and popular method of solving differential equations, especially the boundary value problem. Weighted residual method or variational principles are typically used in determining the expansion coefficients, the former being widely applicable. Weighted residual methods seek to minimise the residuals of the function in the interval of interest. For example, \mathbf{a} is determined by this equation in the interval (0,1)

$$\int_0^1 R_\infty(a_1, u) W_j(u) du = 0 \quad j = 1, 2, 3, \dots, N \quad (2.55)$$

Where \mathbf{W} is a weighted function whose value is \mathbf{W}_j at the collocation point j or in general, \mathbf{a}_1 is determined such that the weighted residuals has a mean value of zero in the volume of the system

$$\int_N R_N(a_1, u) W_j dV = 0 \quad j = 1, 2, 3, \dots, N \quad (2.56)$$

Various methods of weighted residuals are characterised by specific choice of the weight function $W(u)$. The most often used are:

1. The collocation method

Choose the weighting functions to be the dirac delta function

$$W_j(u) = \delta(u - u_j) \quad j = 1, 2, 3, \dots, N \quad (2.57)$$

where \mathbf{u}_j are the \mathbf{N} points in $(0,1)$. This equivalent to

$$R_N(a, u) = 0 \quad j = 1, 2, 3, \dots, N \quad (2.58)$$

Thus the method forces the residual to be zero at \mathbf{N} specified points known as the collocation points. As \mathbf{N} increases, the residual is zero at more points and may ultimately approach zero everywhere in the spatial domain.

Slater (1934) first applied the collocation method to solve differential equations, before developing it into a general method for solving ordinary differential equations (ODE's). Frazer et al (1937) used many trial functions and placed the collocation space where \mathbf{n} becomes very large and the elements (coordinates) of the vectors can be represented as a continuous function of some independent variable.

2. The Sub-domain Method

The weighting functions are chosen to be a set of functions that break the region \mathbf{V} into \mathbf{N} sub-regions \mathbf{V}_j . Choose $W_j(\mathbf{u}) = 1$ inside \mathbf{V}_j and 0 outside \mathbf{V}_j . Divide the range $0 \leq u \leq 1$ into \mathbf{N} subintervals by the interior points

$$u, u_2, \dots, u_{N-1} \quad (u_o, u_N = 1) \quad (2.59)$$

This can be written thus

$$\int_{u_{j-1}}^{u_j} R_N(a, u) du = 0 \quad j = 1, 2, 3, \dots, N \quad (2.60)$$

Which means that the average value of the residual must vanish over each of the $\mathbf{N+1}$ sub-domains. As \mathbf{N} increases, the differential equation is satisfied on the average in smaller and smaller sub-domains and may ultimately approach zero elsewhere.

3. The Method of Moments

The weighting functions are chosen to be the powers of z . $W_j(u)$ is chosen as $u(j-1)$ where $j = 1, 2, 3, \dots, N$, thus

$$\int_1^0 R_N(a, u) u^{j-1} du = 0 \quad (2.61)$$

Other functions $\Phi_j(u)$, $j = 1, 2, 3, \dots, N$ could be used, in fact any arbitrary polynomial of degree $(j - 1)$.

4. The Galerkin Method

Here the weighting functions are chosen to be the basis functions themselves, i.e

$$W_j(u) = T_i = \Phi_k(z) = \frac{\partial y_N}{\partial a_j} \quad (2.62)$$

In this case

$$\int_1^0 R_N(a, u) (1-u) u^{j-1} du = 0 \quad j = 1, 2, 3, \dots, N \quad (2.63)$$

This technique has the advantage that the residual is made orthogonal to each basis function and is therefore the best solution possible in the space made up of the $N + 1$ functions $\Phi_j(z)$. Thus, as $N \rightarrow \infty$, $\mathbf{R}(a, \mathbf{u}) \rightarrow \mathbf{0}$ because it will be orthogonal to every function in a complete set of basis functions, Ray (1981). The Galerkin's method is highly developed for eigenvalue problems. This method is the most accurate of all the various methods of weighted residuals.

5. The least Squares Method

The weighting function is chosen as

$$W_j(u) = \frac{\partial R_N}{\partial a_j} \quad (2.64)$$

$$\int_1^0 R_N(a, u) \frac{\partial R_N}{\partial a_j} du = 0 \quad j = 1, 2, 3, \dots, N \quad (2.65)$$

or determine such that $\int_1^0 [R_N(a, u)]^2 du$ is minimum, which clearly shows why it is referred

to as the method of least squares. Applied to differential equations, the method often leads to cumbersome equations, although Becker (1964) reported applications to complicated problems arising in nuclear reactor engineering.

Of all, the Galerkin method is the most accurate. The Collocation method is however, the most attractive as it has the least complicated expression. A very efficient and accurate

collocation method comparable to the Galerkin method, results when the collocation points are chosen as zeroes of certain orthogonal polynomials (Finlayson, 1972). The method was first developed by Villadsen and Stewart (1967). The orthogonal polynomial can be either Jacobi or Chebychev type.

2.11.7 Polynomoiial Representation of $P_N^{(\alpha,\beta)}(x)$

The Jacobi polynomial $P_N^{(\alpha,\beta)}(x)$ is given by

$$P_N^{(\alpha,\beta)}(x) = \sum_{i=0}^N (-1)^{N-i} \gamma_i x^i \quad (2.66)$$

where γ_0 is taken to be 1 and the remaining N coefficients can be found directly from the orthogonality property,

$$\int x^\beta (1-x)^\alpha P_j(x) dx = 0 \quad j = 1, 2, 3, \dots, N-1 \quad (2.67)$$

or more conveniently

$$\int x^\beta (1-x)^\alpha P_N(x) dx = 0 \quad j = 1, 2, 3, \dots, N \quad (2.68)$$

x^j can be expressed as a linear combination of p_k ($k = 1, 2, \dots, j$). The following set of linear equations for γ_i is derived from equation (2.68),

$$M\gamma = 0 \quad (2.69)$$

$$M_{ji} = \frac{\Gamma(\beta + 1 + i + j)\Gamma(\alpha + 1)}{\Gamma(\alpha + \beta + 2 + i + j)} (-1)^{N-i}, \quad i = 1, 2, 3, \dots, N; \quad j = 1, 2, 3, \dots, N-1 \quad (2.70)$$

since

$$\int_0^1 x^m (1-x)^n dx = \frac{\Gamma(m+1)\Gamma(n+1)}{\Gamma(m+n+2)} \quad (2.71)$$

An alternate simpler method of computing the derivative using Rodrigues' formula from equation (2.66) suggested by Villadsen and Michelsen (1978) is

$$P_N^{(\alpha,\beta)}(x)(1-x)^\alpha x^\beta = \frac{(-1)^N \Gamma(\beta+1)}{\Gamma(N+\beta+1)} \frac{d^N}{dx^N} [(1-x)^{N+\alpha} x^{N+\beta}] \quad (2.72)$$

After computing the N^{th} derivative in equation (2.72) and comparing coefficients of equal powers, γ_i is given by

$$\gamma_i = \binom{N}{i} \frac{\Gamma(N+i+\alpha+\beta+1)\Gamma(\beta+1)}{\Gamma(N+\alpha+\beta+1)\Gamma(i+\beta+1)} \quad (2.73)$$

where

$$\binom{N}{i} = \frac{N!}{i!(N-i)!} \quad (2.65)$$

still, a simpler computational scheme of γ_i is obtained by taking the ratio of γ_i and γ_{i-1} in equation (2.73),

$$\gamma_i = \frac{N-i+1}{i} \frac{N+i+\alpha+\beta}{i+\beta} \gamma_{i-1} \quad (2.74)$$

2.11.7.1 Roots of Polynomial

When the root (zeroes) of any Jacobi polynomial is used as the collocation points, the method is referred to as the orthogonal collocation. The algorithm for the determination of the zeroes of a Jacobi polynomial based on the Newton-Honer Scheme (Villadsen and Michelson, 1978) is as follows:

1. Compute $P_N[x_k^{(i)}]$ using
- $$P_N = [x - g_N(N, \alpha, \beta)] P_{n-1} - h_N(N, \alpha, \beta) P_{n-2} \quad (2.75)$$

where

$$\begin{aligned} g_1 &= \frac{\beta+1}{\alpha+\beta+2} \quad \text{and} \\ g_N &= \frac{1}{2} \left[1 - \frac{\alpha^2 - \beta^2}{(2N + \alpha + \beta - 1)^2 - 1} \right] \quad \text{for } N > 1 \end{aligned} \quad (2.76)$$

$$h_1 = 0$$

$$\begin{aligned} h_2 &= \frac{(\alpha+1)(\beta+1)}{(\alpha+\beta+2)^2(\alpha+\beta+3)} \\ h_N &= \frac{(N-1)(N+\alpha-1)(N+\beta-1)(N+\alpha+\beta-1)}{(2N+\alpha+\beta-1)(2N+\alpha+\beta-2)^2(2N+\alpha+\beta-3)} \quad \text{for } N > 2 \end{aligned} \quad (2.77)$$

The subsequent evaluation of $P_N(x_k)$ is started with $N = 1$ $P_{-1}(x_k)$ arbitrary and $P_o(x_k) = 1$

2. Form a symmetric Tridiagonal matrix T from

$$T_{j,j-1} = T_{j-1,j} = \sqrt{h_j} \quad (2.78)$$

and

$$T_{j,j} = x_k^{(i)} - g_j \quad (2.79)$$

3. Determine the eigenvalues of the matrix using the Quotient Difference algorithm. The method deduces the roots from a table computed from quotients and differences of the equations, just like a difference table.

2.12 THE RIEMANN PROBLEM AND RIEMANN SOLVERS

Having introduced Godunov's (1959) method and obtained the update formula which is based upon the solution of a Riemann problem, it is now necessary to explain what a Riemann problem is. The Riemann problem is defined as an initial value problem of the form

$$U_t + F_x = 0 \quad (2.80)$$

with the initial conditions

$$U(x,0) = \begin{cases} U_L & \dots x < x' \\ U_R & \dots x > x' \end{cases} \quad (2.81)$$

where the initial values may be discontinuous across x' , and equation (2.80) may correspond to a scalar conservation law or a system. The solution of the Riemann problem is problem dependent however the solution to different Riemann problems (corresponding to different choices of F) have certain properties in common. Away from the point x' the constant states U_L and U_R are maintained. These two regions are linked by waves where the number of waves present in the solution is the same as the number of equations in the conservation law, or the number of characteristics. If the wave structure is known then a solution can be found. It is possible to construct exact Riemann solvers which are based on an iterative procedure, however this process is costly. The original Godunov (1959) method involved finding the exact solution to the Riemann problem at each interface. As most of the information obtained from the solution is redundant within the final update, attention has been drawn towards devising approximate Riemann solvers, which can be used within the Godunov (1959) framework. One possibility for doing this is to find an approximation for U^* within the Godunov (1959) flux, Mingham and Causon (1998).

Another approach is to replace the function $\bar{U}(x,t)$ used to definite the cell average values

of U_{i+1}^n , with an approximate solution $\tilde{U}^n(x, t)$ such that the discrete solution is evaluated using

$$U_i^{n+1} = \frac{1}{\Delta x} \int_{x_{i-1/2}}^{x_{i+1/2}} \tilde{U}^n(x, t_{n+1}) dx \quad (2.82)$$

Following the second philosophy, Roe (1981) developed an approximate Riemann solver for the Euler equation for fluid flow in open channels.

2.12.1 Roe-Riemann Solver

The approximate Riemann solver developed by Roe for the Euler equations for the open channels flow is presented. We will also develop a solver for the blood flow equations using the Finite Volume Scheme, the Roe's scheme and the Riemann methods in this work

2.12.2 Roe's Construction

The basis of Roe's method is to construct $\tilde{U}^n(x, t)$ in the relationship

$$U_i^{n+1} = \frac{1}{\Delta x} \int_{x_{i-1/2}}^{x_{i+1/2}} \tilde{U}^n(x, t_{n+1}) dx \quad (2.83)$$

by employing a local linearisation and solving a constant coefficient system of linear conservation laws, with the corresponding flux $\tilde{F}(U) = \tilde{A}\tilde{U}$. In terms of the Riemann problem, the matrix \tilde{A} must depend upon U_L and U_R and the modified conservation law is represented by

$$U_t + \tilde{A}(U_L, U_R)U_x = 0 \quad (2.84)$$

Equation (2.84) is solved exactly, and this corresponds to replacing the original Riemann problem with an approximate Riemann problem. The solution obtained is then an approximate solution to the original conservation law. Using the local linearization allows the theory of constant coefficient linear system to be extended to non-linear problems. The difficulty in extending the linear theory lies in determining an approximate Jacobian, \tilde{A} .

Roe began by defining a series of properties which any suitable choice of $\tilde{A}(U_L, U_R)$ would

need to satisfy. Collectively, these criteria were termed ‘Property U’ and were interpreted by Le Veque (1992) to say that the following conditions should apply

1. $\tilde{A}(U_L, U_R)(U_R - U_L) = F(U_R) - F(U_L)$
2. $\tilde{A}(U_L, U_R)$ is diagonalizable with real eigenvalues
3. $\tilde{A}(U_L, U_R) \rightarrow F'(U)$ smoothly as $U_L, U_R \rightarrow U$

The first condition ensures that if U_L and U_R are connected by a single shock, then the approximate Riemann solution reproduces the exact solution and the Rankine-Hugoniot relationship is satisfied. The second condition ensures that equation (2.84) is both hyperbolic and soluble. Finally the third requirement means that the solution will behave reasonably for smooth solutions. Although an obvious choice of some form of average such as $\tilde{A} = (A_R - A_L)/2$ or $\tilde{A} = (U_R - U_L)/2$ might satisfy the second and third conditions, in general such an average will not meet the first condition. Roe demonstrated how to construct a matrix for the Euler equation that would satisfy Property U. The linear theory is extended to non-linear systems by constructing a matrix \tilde{A} for which

$$\tilde{A}\Delta U = \Delta F$$

Where $\Delta U = U_R - U_L$ (i.e condition 1.) This is equivalent to finding the approximate value that satisfy

$$\Delta U = \sum \tilde{\alpha}_k \tilde{e}_k \quad (2.85)$$

and

$$\Delta F = \sum \tilde{\lambda}_k \tilde{\alpha}_k \tilde{e}_k \quad (2.86)$$

Where $\tilde{\alpha}_k$ corresponds to the strength of the k^{th} wave in the Riemann solution travelling with speed $\tilde{\lambda}_k$ and \tilde{e}_k represent the right eigenvectors of the matrix \tilde{A} with associated eigenvalues also defined by $\tilde{\lambda}_k$. Having generated the approximated quantities the flux at the cell interface can be defined as

$$F_{i+1/2}(U_L, U_R) = \frac{1}{2}(F_L + F_R) - \frac{1}{2} \sum \alpha_k \left| \tilde{\lambda}_k \right| e_k \quad (2.87)$$

2.13 KINETICS OF DRUG METABOLISM

Richard and Mary (2006) explained that drugs are often eliminated by biotransformation and/or excretion into the urine or bile. The liver is the major site for drug metabolism, but specific drugs may undergo biotransformation in other tissues.

- (a) **First-order kinetics:** the metabolic transformation of drugs is catalyzed by enzymes, and most of the reactions obey Michaelis-Menten kinetics:

$$V = \text{rate of drug metabolism} = \frac{V_{\max}[C]}{K_m + [C]} \quad (2.88)$$

In most clinical situations, the concentration of the drug, [C], is much less than the Michaelis constant, K_m , and the Michaelis-Menten equation reduces to

$$V = \text{rate of drug metabolism} = \frac{V_{\max}[C]}{K_m} \quad (2.89)$$

That is, the rate of drug metabolism is directly proportional to the concentration of free drug, and first-order kinetics is observed. This means that a constant fraction of drug is metabolized per unit of time.

- (b) **Zero-order kinetics:** with a few drugs, such as aspirin, ethanol and phenytoin, the doses are very large. Therefore, the [C] is much greater than K_m , and the velocity equation becomes:

$$V = \text{rate of drug metabolism} = \frac{V_{\max}[C]}{[C]} = V_{\max} \quad (2.90)$$

The enzyme is saturated by a high free-drug concentration and the rate of metabolism remains constant over time. A constant amount of drug is metabolized per unit of time.

2.13.1 Kinetics of Continuous Administration

Pharmacokinetics describes the quantitative, time-dependent changes of both the plasma drug concentration and the total amount of drug in the body, following the drug administration by various routes, with the two most common being intravenous (IV) infusion and oral fixed-dose/fixed-time intervals. With continuous IV infusion, the rate of drug entry into the body is constant. In the majority of cases, the elimination of a drug is

first-order; that is, a constant fraction of the agent is cleared per unit of time (Richard and Mary, 2006).

2.14 TESTING KINETIC MODELS

Two problems make the search for the correct mechanism of reaction difficult. First, the reaction may proceed by more than one mechanism, say free radical and ionic, with relative rates that change with conditions. Second, more than one mechanism can be consistent with kinetic data. Resolving these problems is difficult and requires an extensive knowledge of the chemistry of the substances involved. Leaving these aside, let us see how to test the correspondence between experiment and a proposed mechanism that involves a sequence of elementary reactions (Levenspiel, 1999).

2.15 DETERMINING THE ORDER FROM THE EXPERIMENTAL DATA

Sometimes it is possible to determine the order directly from the experimental data though in general this does not happen. Data are rarely as obvious as order can be found and the relation of rate to concentration cannot be determined by inspection

2.15.1 A Straight Forward Graphical Method

In general, the aim is to find just how the rate changes with concentration, is it proportional to [reactant], $[reactant]^2$, $[reactant]^0$, or Michaelis-Menten form. If graphs of rate versus [reactant], $[reactant]^2$, $[reactant]^0$ etc are drawn, then the one which is linear gives the order. This method depends on making guesses as to which orders might fit the results and hoping that the correct is the one of those chosen. If the order is complex, this could be a ‘hit or miss’ procedure, but it illustrates the meaning of order clearly (Levenspiel, 1999).

2.15.2 Log/Log Graphical Procedures

These are completely systematic, and eliminate the necessity of making guesses as to the possible orders. They give the order and rate constant direct from one graph.

$$Rate = k[reactant]^n \quad (2.91)$$

Taking logarithms (to base 10 or base e) of both sides gives

$$\log Rate = \log k + n \log [reactant] \quad (2.92)$$

And the plot of log rate versus log [reactant] should give linear with slope = n and intercept = $\log k$. Hence k and n can be found.

The conclusion follows that the rate depends in some way on [reactant] remaining,

$$\text{rate} \propto [\text{reactant}]^n \quad (2.93)$$

Where n is a number which states exactly how the rate depends on the [reactant]. It is called the order. From this,

$$\text{rate} = k [\text{reactant}]^n \quad (2.94)$$

Where k is a constant of proportionality called the rate constant:

If $n = 1$, the reaction is first order.

If $n = 2$ the reaction is second order.

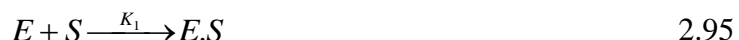
If $n = 3/2$, the reaction is three-half order.

If $n = 0$, it is zero order.

The significance of the Rate Constant as opposed to the Rate is that: for all orders, except zero order, the rate of reaction varies with the concentration and is useless as a means of either quantifying reactions or comparing them. In contrast, the rate constant is a constant at a given temperature and is independent of concentration. It can be used to quantify or compare reactions. Also, if the rate constant and the order are known, then it is easy to calculate rate for any concentration. The drawback of the methods just mentioned is that the SITT data do not have rates and calculating for all the data is not feasible as the rate for all orders will be different at different concentrations, hence difficult to evaluate the correct order (Margaret, 2004).

2.16 KINETICS OF ENZYME CATALYZED REACTIONS

An enzyme, E , is a protein or protein-like substance with catalytic properties. A substrate, S , is the substance that is chemically transformed at an accelerated rate because of the action of the enzyme on it. An important property of enzymes is that they are specific in that one enzyme can catalyzed only one reaction. Since the utilization of glucose by the body cells to produce energy is the reaction that is promoted by enzymes actions, the kinetics of such kind of reaction can be described as follows (Fogler, 2005).





Where E is enzyme urease, S is the substrate, W is water, P is ammonia and carbon dioxide and E.S is enzyme-substrate complex.

The rate of disappearance of the substrate $-r_s$ is

$$-r_s = k_1(E)(S) - k_2(E.S) \quad 2.98$$

The net rate of formation of the enzyme-substrate complex is

$$r_{E.S} = k_1(E)(S) - k_2(E.S) - k_3(W)(E.S) \quad 2.99$$

Note from the reaction sequence that the enzyme is not consumed by the reaction. The total concentration of the enzyme in the system, (E_t), is constant and equal to the sum of the concentrations of the free or unbounded enzyme E and the enzyme-substrate complex E.S.

$$(E_t) = (E) + (E.S) \quad 2.100$$

Rearranging Equation (2.100), the enzyme concentration becomes

$$(E) = (E_t) - (E.S) \quad 2.101$$

Substituting Equation (2.101) into Equation (2.99) and using pseudo steady state hypothesis for the enzyme complex gives

$$r_{E.S} = 0 = k_1[(E_t) - (E.S)](S) - k_2(E.S) - k_3(E.S)(W) \quad 2.102$$

Solving for $(E.S)$ yields

$$(E.S) = \frac{k_1(E_t)(S)}{k_1(S) + k_2 + k_3(W)} \quad 2.103$$

Next substituting Equation (2.101) into Equation (2.98) yields

$$-r_s = k_1[(E_t) - (E.S)](S) - k_2(E.S) \quad 2.104$$

Substracting Equation (2.102) from Equation (2.104), we get

$$-r_s = k_3(W)(E.S) \quad 2.105$$

Substituting for $(E.S)$ gives the final form of the rate law as

$$-r_s = \frac{k_1 k_3(W)(E_t)(S)}{k_1(S) + k_2 + k_3(W)} \quad 2.106$$

Note that E_t is the total concentration of enzyme with typical units (kmol/m^3).